

**INSTITUTO DE QUÍMICA**

**PROGRAMA DE PÓS-GRADUAÇÃO EM GEOCIÊNCIAS - GEOQUÍMICA**

**JOÃO MARCELO BALLALAI**

**TWO-PHASE AMOC RECOVERY CONTROLLED BY OCEAN-ATMOSPHERIC  
COUPLING GATEWAY IN THE WESTERN SOUTH ATLANTIC DURING THE  
LAST INTERGLACIAL**

**UNIVERSIDADE  
FEDERAL  
FLUMINENSE**

**NITERÓI**

**2019**

JOÃO MARCELO BALLALAI

**TWO-PHASE AMOC RECOVERY CONTROLLED BY OCEAN-ATMOSPHERIC  
COUPLING GATEWAY IN THE WESTERN SOUTH ATLANTIC DURING THE  
LAST INTERGLACIAL**

Dissertação apresentada ao Curso de Pós-Graduação em Geociências da Universidade Federal Fluminense, como requisito parcial para a obtenção do Grau de Mestre. Área de Concentração: Geoquímica Ambiental.

Orientadora:

Prof.<sup>a</sup> Dr.<sup>a</sup> Ana Luiza Spadano Albuquerque

Coorientador:

Dr. Thiago Pereira dos Santos

NITERÓI

2019

Ficha catalográfica automática - SDC/BGQ  
Gerada com informações fornecidas pelo autor

B188t Ballalai, João  
Two-phase AMOC recovery controlled by ocean-atmospheric coupling gateway in the western South Atlantic during the Last Interglacial / João Ballalai ; Ana Luiza Spadano Albuquerque, orientadora ; Thiago Pereira dos Santos, coorientador. Niterói, 2019.  
71 f. : il.

Dissertação (mestrado)-Universidade Federal Fluminense, Niterói, 2019.

DOI: <http://dx.doi.org/10.22409/PPG-Geo.2019.m.14214968794>

1. Vazamento das Agulhas. 2. Giro subtropical do Atlântico Sul. 3. Transferência de calor inter-hemisférica. 4. Produção intelectual. I. Spadano Albuquerque, Ana Luiza, orientadora. II. Santos, Thiago Pereira dos, coorientador. III. Universidade Federal Fluminense. Instituto de Química. IV. Título.

CDD -

JOÃO MARCELO BALLALAI

**TWO - PHASE AMOC RECOVERY CONTROLLED BY OCEAN-  
ATMOSPHERE COUPLING GATEWAY IN THE WESTERN  
SOUTH ATLANTIC DURING THE LAST INTERGLACIAL**

Dissertação apresentada ao Curso de Pós - Graduação  
em Geociências da Universidade Federal Fluminense,  
como requisito parcial para a obtenção do **Grau  
de Mestre**. Área de Concentração: **Geoquímica  
Ambiental**.

Aprovada em Fevereiro de 2019.

**BANCA EXAMINADORA**



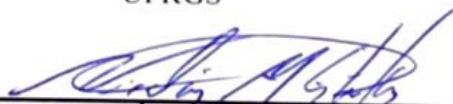
PROF. DRa. ANA LUIZA SPADANO ALBUQUERQUE  
ORIENTADOR/UFF



DR. THIAGO PEREIRA DOS SANTOS  
COORIENTADOR/UFF



PROF. Dra. MARIA ALEJANDRA GOMEZ PIVEL  
UFRGS



PROF. DR. NICOLÁS MISALIDIS STRIKIS  
UFF



PROF. DRa. CARLA REGINA ALVES CARVALHO  
UFF

## **ACKNOWLEDGEMENTS**

This dissertation was not done by just one person, neither two. A lot of people had a crucial role during the process to build up what will be presented in the next pages. Because of that, I would like to say really thank you to all that participated during this stage of my life.

I thank my parents who always give me all support needed and believe in my work, in my honesty and always keep continuous encouragement.

I really thank my two supervisors, Ana and Thiago for their help, support and a lot of patience during the process. I'm really thankful to all knowledge and opportunities that you guys gave me, without your help it couldn't be possible.

I thank all integrant of Laboratório de Oceanografia Operacional e Paleoceanografia (LOOP-UFF) that always were willing and helped me. Especially to Caio that always was by my side, supporting and tranquilizing me since the begging.

I would like to thank all professors, staff crew of the Departamento de Geoquímica for all knowledge and dedication to your students.

I thank my partner and life mate Letícia Vianna to supporting me and to be always by my side all the time. You are really special, I believe us.

I thank all my friends, especially those who finished the bachelors with me. From UNIRIO to life.

I would like to especially thank my father, who always believe in this path and dream to this moment. I know that you would be proud.

I thank CNPq and CAPES for the financial support granting the scholarship over the period of this master's degree.

## RESUMO

O processo de retroflexão da corrente das Agulhas está associado à formação de anéis e filamentos causados por instabilidades na corrente, onde parte de suas águas invade o Atlântico Sul sendo incorporadas no giro subtropical (do inglês, *Subtropical Gyre*, STG). As águas do vazamento das Agulhas (do inglês, *Agulhas Leakage*, AL) são uma importante fonte de densidade que força a Célula de Revolvimento Meridional do Atlântico (do inglês, *Atlantic Meridional Overturning Circulation*, AMOC) e as massas d'água associadas a serem carreadas para a região subpolar do Atlântico Norte como parte superior da circulação meridional. A entrada de calor e sal através dessa rota desempenha um papel importante na manutenção da salinidade, reestabelecendo a força e a estabilidade da circulação. A intensificação do AL durante as Terminações glaciais tem sido proposta como um mecanismo necessário para que haja a retomada do modo interglacial da AMOC e é parte fundamental para que ocorram as mudanças climáticas que precedem os processos de deglaciação. No entanto, a falta de registros mostrando a progressão do sinal do AL em seu curso e, a grande diferença temporal existente entre a intensificação do vazamento e a retomada da AMOC coloca em dúvida este mecanismo. Este trabalho tem como objetivo central avaliar a extensão e o papel do AL no retorno da AMOC ao redor da Terminação glacial II. Foram desempenhadas análises da razão Mg/Ca através de ICP-OES aplicadas em testas do foraminífero planctônico da espécie *Globorotalia inflata*, afim de reconstituir em escala milenar as paleotemperaturas e paleosalinidades de termoclina da porção oeste do Atlântico Sul. Durante a Terminação glacial II, as águas do AL recircularam na região subtropical do Atlântico Sul até serem abruptamente liberadas em dois pulsos para o Atlântico Norte. Os dois pulsos ocorreram de forma sincrônica com os dois intervalos de reativação da AMOC registrados em 129 ka AP no Mar do Labrador, e depois em 124 ka AP no Mar Nórdico durante parte do Último Interglacial (MIS 5e), duas regiões produtoras de Água Profunda do Atlântico Norte (APAN). O mecanismo proposto neste trabalho sugere que a posição da bifurcação da Corrente Sul Equatorial (CSE) e a expansão e contração das células subtropicais são moduladas pela posição da Zona de Convergência Intertropical (do inglês, *Intertropical Convergence Zone*, ITCZ). Durante as Terminações glaciais, a ITCZ estaria em sua posição mais a sul, favorecendo o transporte via Corrente do Brasil e, consequentemente, recirculando as águas do AL no STG. No início do MIS 5e, a ITCZ se deslocaria para sua posição mais ao norte e favoreceria o transporte via Corrente Norte do Brasil (CNB), liberando essas águas em direção ao Atlântico Norte. Essa partição da energia entre os ramos norte e sul da corrente de contorno oeste do Atlântico Sul tem um importante papel na comunicação do sinal entre os hemisférios e na modulação da intensidade da AMOC. Nossa hipótese propõe conectar a intensificação do AL com o retorno da AMOC em duas fases durante parte do Último Interglacial. A bifurcação da CSE atua como um portão oceânico-atmosfera mediado pelo posicionamento médio da ITCZ que controla a transmissão para o norte das anomalias de salinidade através do Equador, permitindo que o fluxo de águas salinas do AL chegue aos locais de convecção de águas profundas no Hemisfério Norte.

**Palavras-chave:** Vazamento das Agulhas. Termoclina no Atlântico Sul. Giro subtropical do Atlântico Sul. Transferência de calor inter-hemisférica.

## ABSTRACT

The Agulhas current retroflection process is linked to the formation of edges and filaments (Agulhas rings) through instabilities in the current, where part of these waters invades South Atlantic being incorporated into subtropical gyre (STG). The Agulhas Leakage (AL) provides an important source of density forcing the Atlantic meridional overturning circulation (AMOC) and their related waters-masses be carried towards the subpolar North Atlantic as the upper limb of the meridional circulation. The input of heat and salt throughout this route plays a key role in maintaining salinity, recovering the strength and stability of meridional circulation. The AL intensification during glacial Terminations has long been proposed as a required mechanism to return the AMOC to its interglacial mode and has a crucial role to occur the climate changes that precedes the deglaciation processes. However, the lack of records showing the downstream evolution of the AL signal and the large temporal differences between AL intensification and AMOC resumption cast doubt on this mechanism. The main objective of this study is to evaluate the extension and the role of the AL on AMOC recovery during glacial Termination II. Mg/Ca analyses were performed using ICP-OES applied in foraminiferal tests of *Globorotalia inflata* specie, aiming to reconstruct millennial-scale thermocline paleotemperatures and paleosalinities from the western South Atlantic. During glacial Termination II, AL waters recirculated in the surface and thermocline subtropical South Atlantic until they were abruptly released to the North Atlantic in two pulses. These pulses were synchronous to two intervals of AMOC recovering recorded in 129 ka BP in the Labrador Sea, and after in 124 ka BP in the Nordic Sea during part of the Last Interglacial, both sites of North Atlantic Deep Water production. The mechanism proposed here suggests that the position of the South Equatorial current (SEC) bifurcation and the subtropical cells expansion and contraction are modulated by the Intertropical Convergence Zone (ITCZ) positioning. During glacial Terminations the ITCZ is positioned in the further southern position favoring the transport via Brazil Current, hence recirculating AL waters in the STG. At early MIS 5e the ITCZ shift to further northern positioning and favors the transport via North Brazil Current, releasing these waters toward North Atlantic. This energy partition between the northward and the southward branch of the South Atlantic western contour currents has an important role in the communication of the signal between southern and northern hemisphere and to modulate the AMOC intensity. Our hypothesis proposes connect AL intensification and the two-phase AMOC recovery during the Last Interglacial period. The SEC bifurcation acts as an ocean-atmospheric gateway controlling the northward transmission of salty anomalies from tropical regions in South Atlantic across the Equator, allowing the flux of dense AL waters to reach the sites of deep-water convection in the North Hemisphere.

**Keywords:** Agulhas Leakage. South Atlantic thermocline. South Atlantic subtropical gyre. Interhemispheric heat transfer.

## LIST OF FIGURES

<b>Figure 1</b> - Multiple observed indicators of a changing global climate on Earth system. A: Annually and globally averaged combined land and ocean surface temperature anomalies relative to the average over the period 1986 to 2005. Colours indicate different data sets. B: Annually and globally averaged sea level change relative to the average over the period 1986 to 2005 in the longest-running dataset. Colours indicate different data sets. All datasets are aligned to have the same value in 1993, the first year of satellite altimetry data (red). Where assessed, uncertainties are indicated by coloured shading C: Atmospheric concentrations of the greenhouse gases carbon dioxide (CO <sub>2</sub> , green), methane (CH <sub>4</sub> , orange) and nitrous oxide (N <sub>2</sub> O, red) determined from ice core data (dots) and from direct atmospheric measurements (lines). D: Global anthropogenic CO <sub>2</sub> emissions from forestry and other land use as well as from burning of fossil fuel, cement production and flaring. Cumulative emissions of CO <sub>2</sub> from these sources and their uncertainties are shown as bars and whiskers, respectively, on the right hand side. The global effects of the accumulation of CH <sub>4</sub> and N <sub>2</sub> O emissions are shown in panel C. These indicators put in evidence the different impacts since the intensification of human activities (IPCC, 2014). .....	15
<b>Figure 2</b> - Global thermohaline circulation. Red curves indicading the warm-water route and blue curves indicating the cold-water routes of the global circulation. ....	16
<b>Figure 3</b> - AMOC circulation emphasizing the transport through the Atlantic basin and reaching both sites of North Atlantic Deep Water (NADW) production (BEAL et al., 2011) .....	17
<b>Figure 4</b> - The main foraminifera specie employed in this study: <i>Globorotalia inflata</i> (250-300 µm) .....	20
<b>Figure 5</b> - Schematic representation of the Agulhas system and invasion of Agulhas waters into the South Atlantic. Position of subtropical front and emphasis on the intensification of .....	



westerly winds as a oceanic gateway mechanism leading the Indian-Atlantic connection (BEAL et al., 2011).....	25
<b>Figure 6</b> - Schematic example of surface currents in the tropical South Atlantic (from PETERSON; STRAMMA, 1991).....	27
<b>Figure 7</b> - Map of the South Atlantic surface circulation (modified from Peterson and Stramma, 1991) showing the spatial distribution of sea surface temperature (SST) and the position of core GL-1090. Thick black lines represent the main surface currents in South Atlantic. AL: Agulhas Leakage, BC: Brazil Current, MC: Malvina Current, NBC: North Brazil Current, SAC: South Atlantic Current, SEC: South Equatorial Current and SECC: South Equatorial Countercurrent. Dashed white line shows the austral summer mean position of Intertropical Convergence Zone (ITCZ). .....	32
<b>Figure 8</b> - Alignment between Santos Basin surface $\delta^{18}\text{O}_{\text{IVF-SW}}$ with records of Asian Monsoon from Sanbao Cave with their respective radiometrically $^{230}\text{Th}$ ages (WANG et al., 2008). The new age model of core GL-1090 (green) produces slightly younger ages across the transition to the Last Interglacial compared with the previous one (blue). Grey bar highlights the weak Asian Monsoon period correspondent to Heinrich stadial 11 and yellow bar the transition to strong Asian Monsoon at the onset of the Last Interglacial. ....	34
<b>Figure 9</b> - Comparison between original (left) (SANTOS et al., 2017a) and new (right) Bayesian age-depth model of core GL-1090. The main features of sedimentation rate were preserved but the uncertainty was significantly reduced around the period of interest for this study. ....	35
<b>Figure 10</b> - Comparison between benthic $\delta^{18}\text{O}$ of cores GL-1090 (black) (SANTOS et al., 2017a) and ODP1063 (pink) (DEANEY; BARKER; FLIERDT, 2017). The shift to low $\delta^{18}\text{O}$ during peak MIS 5e occurred approximately 3.6 kyr earlier in the North Atlantic core ODP1063. ....	36

**Figure 11** - Evolution of Santos Basin thermocline proprieties from the Termination II (TII) to the last glacial inception. A: *Globorotalia inflata* (250 – 300  $\mu\text{m}$ )  $\delta^{18}\text{O}$  ref. 1. B: *Globorotalia inflata* (250 – 300  $\mu\text{m}$ ) Mg/Ca (this study). C: Thermocline temperature derived from *Globorotalia inflata* Mg/Ca applying the calibration equation of Cléroux et al. (2008) given by  $[\text{Mg}/\text{Ca} = 0.71 \exp 0.06 \cdot (T)]$ . D: Thermocline  $\delta^{18}\text{O}_{\text{IVF-SW}}$  reconstructed with *Globorotalia inflata*  $\delta^{18}\text{O}$  and Mg/Ca temperature. Error bar is relative to  $1\sigma$ . Thermocline temperature and  $\delta^{18}\text{O}_{\text{IVF-SW}}$  (panels C and D) are presented with a three-point running average (thick lines). Grey dashed lines indicate the boundary between Marine Isotope Stage 6-5e and 5e-5d. Marine isotope stages and TII are indicated at the bottom of the panel..... 41

**Figure 12** - Evolution of the surface and thermocline eastern (Walvis Ridge) and western (Santos Basin) South Atlantic temperature and ice-volume free seawater stable oxygen isotopic composition ( $\delta^{18}\text{O}_{\text{IVF-SW}}$ ) during the Marine Isotope Stage (MIS) 6/5e transition. A and B: Surface temperatures from cores GL-1090 (A, Santos Basin) (SANTOS et al., 2017a) and 64PE-174P13 (B, Walvis Ridge) (SCUSSOLINI et al., 2015) based on Mg/Ca of *Globigerinoides ruber*. C and D: Thermocline temperatures from cores GL-1090 (C, Santos Basin - this study) and 64PE-174P13 (D, Walvis Ridge) (SCUSSOLINI et al., 2015) based on Mg/Ca of *Globorotalia inflata* and *Globorotalia truncatulinoides*, respectively. E and F: Surface  $\delta^{18}\text{O}_{\text{IVF-SW}}$  from cores GL-1090 (E, Santos Basin) (SANTOS et al., 2017b) and 64PE-174P13 (F, Walvis Ridge) (SCUSSOLINI et al., 2015) estimated through Mg/Ca and  $\delta^{18}\text{O}$  of *G. ruber*. G and H: Thermocline  $\delta^{18}\text{O}_{\text{IVF-SW}}$  from cores GL-1090 (G, Santos Basin - this study) and 64PE-174P13 (H, Walvis Ridge) (SCUSSOLINI et al., 2015) estimated through Mg/Ca and  $\delta^{18}\text{O}$  of *G. inflata* and *G. truncatulinoides*, respectively. All records are depicted by the original data (dots and thin line) and the respective three-point running mean (thick line). Grey vertical dashed lines indicate the boundary between MIS 6/5e and 5e/5d. Grey vertical bars on the right-hand panel highlight the interval of surface and thermocline

salinification in the eastern and western South Atlantic. MIS and Termination II (TII) are indicated in the bottom of both panels. .... 44

**Figure 13** -  $\Delta\delta^{18}\text{O}_{\text{IVF-SW}}$  gradient between the upper western and eastern South Atlantic. A: Subtraction of zero-mean normalization of surface  $\delta^{18}\text{O}_{\text{IVF-SW}}$  of core GL-1090 (this study) and 64PE-174P13 (SCUSSOLINI et al., 2015) to generate the  $\Delta\delta^{18}\text{O}_{\text{IVF-SW}}$ . For this case, both cores consider *Globigerinoides ruber* as the suitable species to record surface ocean properties. B: Subtraction of zero-mean normalization of thermocline  $\delta^{18}\text{O}_{\text{IVF-SW}}$  of core GL-1090 (this study) and 64PE-174P13. This estimation takes into account *Globorotalia inflata* for core GL-1090 and *Globorotalia truncatulinoides* for core 64PE-174PE. Either species tend to record the conditions of thermocline, although *G. truncatulinoides* is usually assumed as a deeper thermocline dwelling compared with *G. inflata*. Yellow bar highlights the interval of the Last Interglacial when the two abrupt freshening of the Santos Basin occurred..... 46

**Figure 14** - Surface and thermocline ice-volume free seawater  $\delta^{18}\text{O}$  ( $\delta^{18}\text{O}_{\text{IVF-SW}}$ ) of the South Atlantic and the Atlantic Meridional Overturning Circulation (AMOC) resumption during the early- and mid-Last Interglacial. A: Ice rafted debris (IRD) from core ODP1063 (DEANEY; BARKER; FLIERDT, 2017). B: Sea surface temperatures (SST) based on Mg/Ca of *Neogloboquadrina pachyderma* (sinistral) from core MD03-2664 (IRVALI et al., 2016). C: June 21 insolation at 65 °N (BERGER, 1978). D: Relative abundance of polar planktic foraminifera *N. pachyderma* (sinistral) from core MD03-2664 (IRVALI et al., 2016). E: Warm planktic foraminifera species (*Globigerinoides ruber* + *Globigerinoides sacculifer*) from core ODP1063 (DEANEY; BARKER; FLIERDT, 2017). F: Neodymium isotopic composition ( $\epsilon\text{Nd}$ ) from core ODP 1063 (pink (DEANEY; BARKER; FLIERDT, 2017) and purple (BÖHM et al., 2015). G: *Cibicides wuellerstorfi*  $\delta^{18}\text{O}$  from core ODP1063 (DEANEY; BARKER; FLIERDT, 2017). H: Surface  $\delta^{18}\text{O}_{\text{IVF-SW}}$  from core GL-1090 estimated through Mg/Ca and  $\delta^{18}\text{O}$  of *G. ruber* (SANTOS et al., 2017a). I: Sortable silt from cores NEAP-18K

(blue) (HALL et al., 1998) and ODP983 (pink) (DEANEY; BARKER; FLIERDT, 2017). J: *C. wuellerstorfi*  $\delta^{13}\text{C}$  from cores ODP1063 (green) (DEANEY; BARKER; FLIERDT, 2017), GL-1090 (black) (SANTOS et al., 2017a) and ODP U1304 (orange) (HODELL et al., 2009). K: Thermocline  $\delta^{18}\text{O}_{\text{IVF-SW}}$  of core GL-1090 estimated through Mg/Ca and  $\delta^{18}\text{O}$  of *Globorotalia inflata* (this study). Marine isotope stages and Termination II (TII) are indicated in the bottom of both panels. Grey and yellow vertical bars indicate the peak in salt accumulation and salt release periods, respectively. Note that grey and yellow bars highlight different periods in the left-hand and right-hand panels. .... 48

**Figure 15** - Schematic position of the Intertropical Convergence Zone (ITCZ), the surface circulation of the South Atlantic and sea surface salinity evolution during Termination II (TII) (A and B) and the early Last Interglacial (C and D). Yellow dots show the position of GL-1090 (this study) and other cores discussed here (ODP1058 is not shown). Panels B and D show GL-1090 surface  $\delta^{18}\text{O}_{\text{IVF-SW}}$  (SANTOS et al., 2017a) together with Sanbao Cave  $\delta^{18}\text{O}$  (WANG et al., 2008) as an indicator of the ITCZ fluctuations across the penultimate glacial-interglacial transition. Note that in A and B the southern ITCZ results in a northern position of the South Equatorial Current (SEC) bifurcation, a stronger Brazil Current (BC), a weaker North Brazil Current (NBC) and the storage of the salty Agulhas Leakage (AL) waters within the South Atlantic subtropical gyre (area in red). The scenario rapidly changed at the onset of the Last Interglacial (C and D) when a northern ITCZ led to a stronger NBC and a weaker BC, decreasing the salinity of the area highlighted in blue. .... 52

**Figure 16** - South Atlantic thermocline temperature and ice-volume free seawater  $\delta^{18}\text{O}$  ( $\delta^{18}\text{O}_{\text{IVF-SW}}$ ) from Termination II (TII) to the last glacial inception (Marine Isotope Stage 5d) compared with North Atlantic paleoclimate reconstructions. A: sortable silt from core NEAP-18K (HALL et al., 1998). B: Relative abundance of polar planktic foraminifera *Neoglobobulimina pachyderma* (sinistral) from core MD03-2664 (IRVALI et al., 2016). C:

Thermocline temperature from core ODP1058 based on Mg/Ca of *Globorotalia truncatulinoides* (sinistral) (BAHR et al., 2013). D: Thermocline  $\delta^{18}\text{O}_{\text{IVF-SW}}$  from core ODP 1058 estimated through Mg/Ca and  $\delta^{18}\text{O}$  of *G. truncatulinoides* (sinistral) (BAHR et al., 2013). E: Thermocline temperature from core GL-1090 (Santos Basin) based on Mg/Ca of *Globorotalia inflata* (this study). F: Thermocline  $\delta^{18}\text{O}_{\text{IVF-SW}}$  from core GL-1090 estimated through Mg/Ca and  $\delta^{18}\text{O}$  of *G. inflata* (this study). Marine isotope stages and TII are indicated in the bottom of the panel. Yellow bar highlights the period of full deep-water convection in both the Labrador and Nordic Seas. When this condition was achieved salt and heat were removed from the western South Atlantic thermocline. .... 54

**Figure 17** - Source: Source: Developed by the author, 2019..... 55

## SUMMARY

<b>1</b>	<b>GENERAL INTRODUCTION.....</b>	<b>14</b>
	<b>PALEOCEANOGRAPHIC DATA FROM LAST INTERGLACIAL PERIOD AND THE CURRENT CLIMATE STUDIES: A CONTRIBUTION TO SOCIETY .....</b>	<b>14</b>
<b>2</b>	<b>OBJECTIVES .....</b>	<b>19</b>
<b>3</b>	<b>LITERATURE REVIEW .....</b>	<b>20</b>
3.1	THE USE OF PLANKTIC FORAMINIFERA APPLIED TO PALEOTEMPERATURE AND SALINITY RECONSTRUCTIONS.....	20
3.1.1	Stable oxygen isotope ( $\delta^{18}\text{O}$ ) applied in paleoceanographic studies.....	20
3.1.2	Magnesium to calcium ratio (Mg/Ca) and derived oxygen isotope of seawater ( $\delta^{18}\text{O}_{\text{sw}}$ )	21
3.2	THE ROLE OF AGULHAS LEAKAGE ON GLACIAL TERMINATIONS.....	22
3.3	THE SOUTH ATLANTIC SUBTROPICAL GYRE .....	26
<b>4</b>	<b>DISCUSSION .....</b>	<b>28</b>
4.1	LAST INTERGLACIAL INTER-HEMISPHERIC TRANSMISSION OF AGULHAS LEAKAGE CONTROLLED BY THE WESTERN SOUTH ATLANTIC.....	28
4.1.1	Introduction.....	28
4.1.2	Study Area .....	30
4.1.3	Material and Methods.....	32
4.1.3.1	GI-1090 Sampling .....	33
4.1.3.2	Age Model.....	33
4.1.3.3	Calculation of thermocline temperature and ice-volume free seawater $\delta^{18}\text{O}$ .....	36
4.1.4	Results.....	39
4.1.4.1	Thermocline temperature and ice volume-free seawater oxygen isotopic evolution in the western South Atlantic .....	39

<b>4.1.5 Discussion .....</b>	<b>42</b>
4.1.5.1 Salinification of the upper subtropical South Atlantic associated with the strengthening of the Agulhas Leakage.....	42
4.1.5.2 Two-phase abrupt freshening of the western South Atlantic and AMOC resumption	45
4.1.5.3 The role of tropical ocean-atmosphere coupling in the Atlantic inter-hemispheric exchange of salt and heat.....	50
<b>4.1.6 Conclusions.....</b>	<b>55</b>
<b>4.1.7 References.....</b>	<b>56</b>
<b>5 GENERAL CONCLUSIONS AND FUTURE PERSPECTIVES .....</b>	<b>64</b>
<b>6 REFERENCES.....</b>	<b>66</b>

## **1 GENERAL INTRODUCTION**

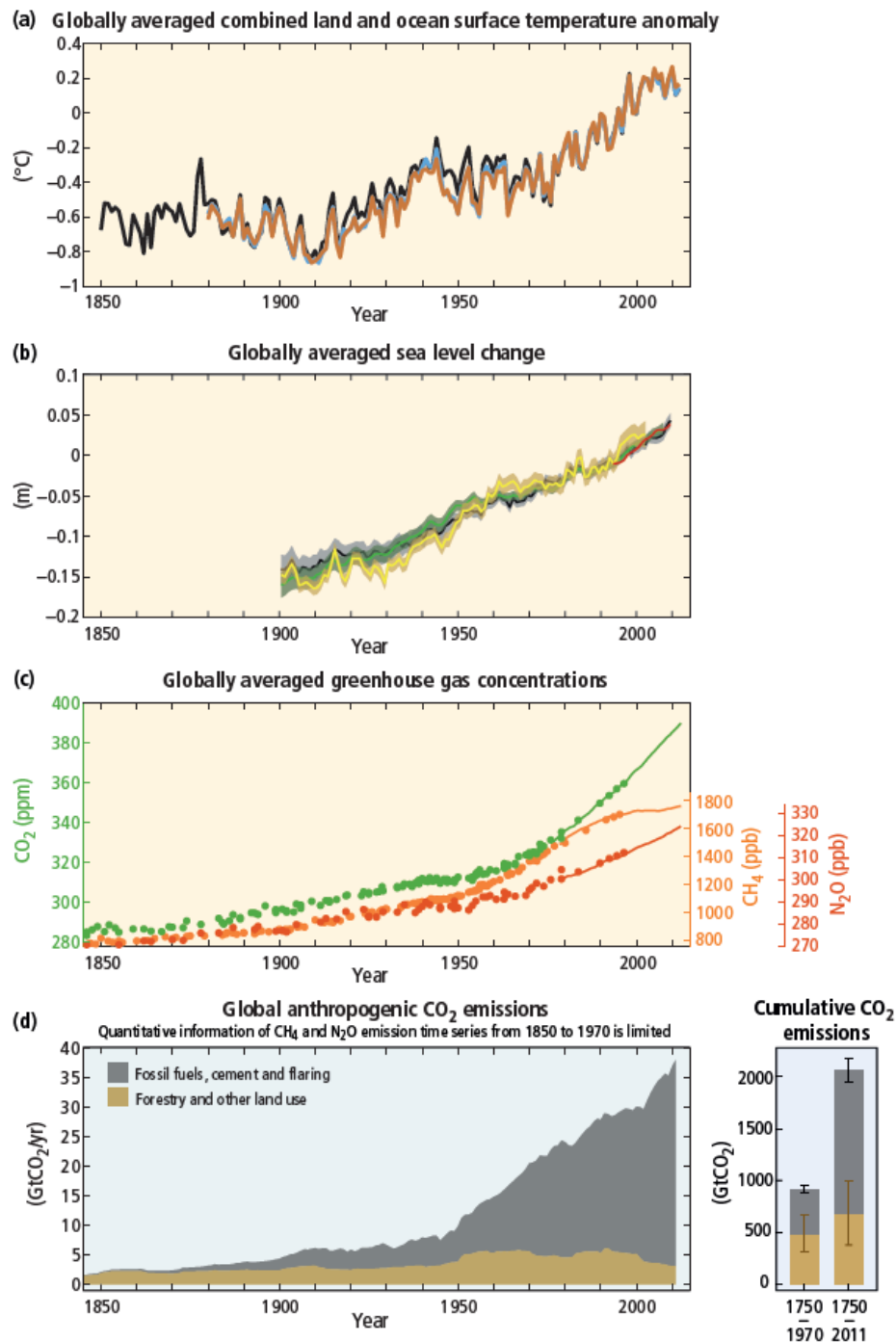
### **PALEOCEANOGRAPHIC DATA FROM LAST INTERGLACIAL PERIOD AND THE CURRENT CLIMATE STUDIES: A CONTRIBUTION TO SOCIETY**

Climatic studies are topics that appears with great urgency to society due to anthropogenic climate change effects on Earth's climatic system. Changes in the past occurred for natural reasons; some of them well understood and others still appear to be in the process of being unraveled. Today Earth's climate is warming and it is clear that humans are a major cause of this change. Many of the observed changes are unprecedented over decades to millennia, the atmosphere and ocean have warmed, the amounts of snow and ice have diminished, sea level has risen, and the concentrations of greenhouse gases have increased (Figure 1).

These effects are responses to the Earth's system causing changes on climate and by modifying the atmosphere and ocean dynamics in the Earth's climatic system. These relationships are fundamental causing different forcing (drive change) and responses (effects) to the climate. The oceans have a crucial role due to their capability to store and distribute energy around the globe through thermohaline circulation (Figure 2). Changes in the ocean-atmospheric dynamics and patterns can have a catastrophic impact on the Earth's system (IPCC, 2014).

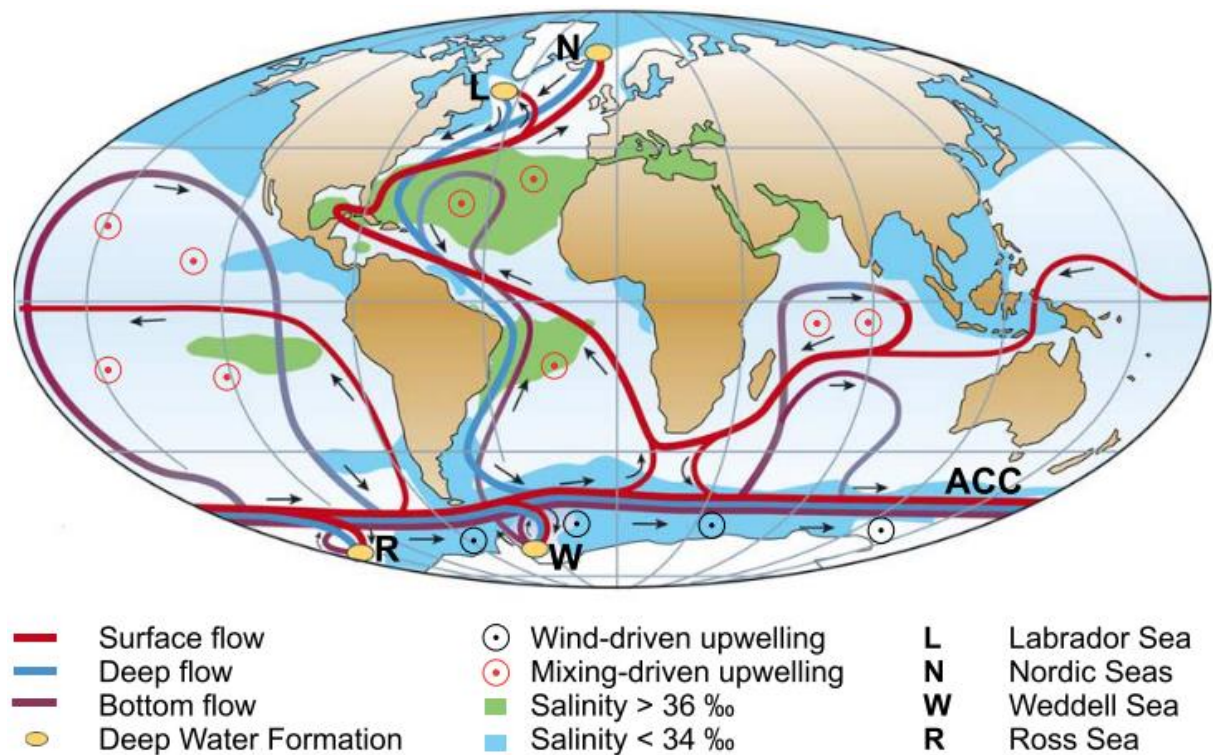


**Figure 1** - Multiple observed indicators of a changing global climate on Earth system. **A:** Annually and globally averaged combined land and ocean surface temperature anomalies relative to the average over the period 1986 to 2005. Colours indicate different data sets. **B:** Annually and globally averaged sea level change relative to the average over the period 1986 to 2005 in the longest-running dataset. Colours indicate different data sets. **C:** Atmospheric concentrations of the greenhouse gases carbon dioxide ( $\text{CO}_2$ , green), methane ( $\text{CH}_4$ , orange) and nitrous oxide ( $\text{N}_2\text{O}$ , red) determined from ice core data (dots) and from direct atmospheric measurements (lines). **D:** Global anthropogenic  $\text{CO}_2$  emissions from forestry and other land use as well as from burning of fossil fuel, cement production and flaring. These indicators put in evidence the different impacts since the intensification of human activities (IPCC, 2014).



Source: IPCC, 2014.

**Figure 2** - Global thermohaline circulation. Red curves indicating the warm-water route and blue curves indicating the cold-water routes of the global circulation.

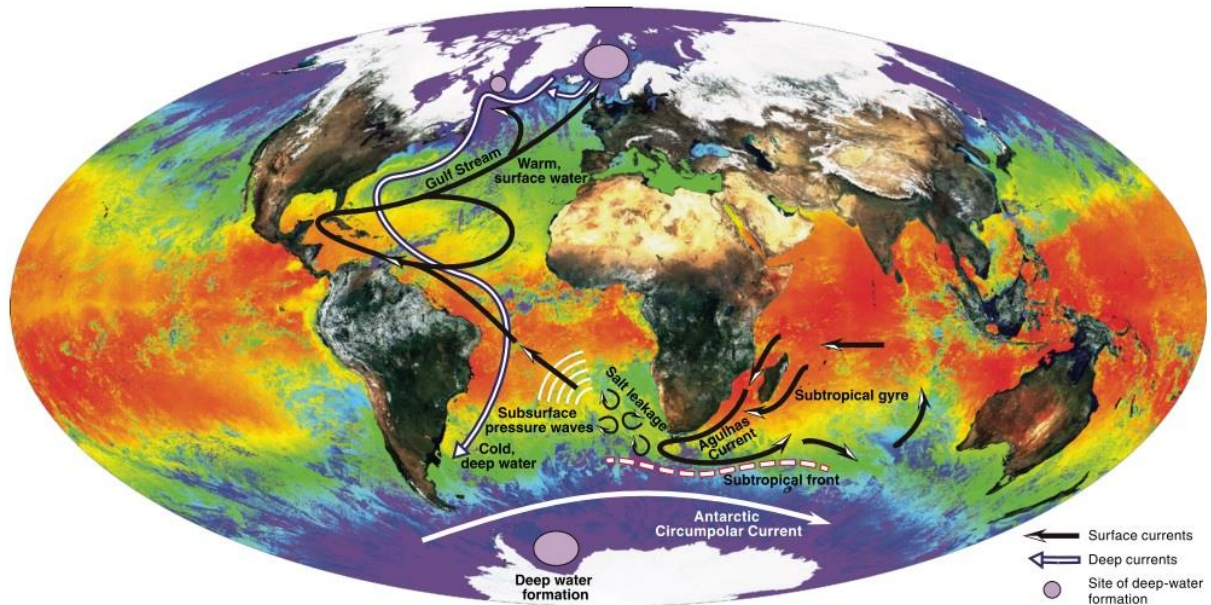


Source: KUHNBRODT et al. 2007 (adapted from RAHMSTORF, 2002).

During the last decades, discussions about the global warming or the collapse of the thermohaline circulation and, hence the Atlantic Meridional Overturning Circulation (AMOC – Figure 3) energy transport, were mainly restricted to the academic society. Nowadays, due to controversial discussions around the anthropogenic impacts on earth's climatic system, the awareness with climate change comes up in a public debate, arising as a contemporary needing of humanity. According to the Intergovernmental Panel on Climate Change (IPCC) report, evidences that climate is indeed undergoing significant variability and suffering big changes, like the increases of global temperature in the oceans e.g. (YIN et al., 2018) and sea level rise during the last century e.g. (MURRAY-WALLACE, 2013), bring into discussion the problematic and emphasize the public's increased concern of the global physical changes and the Earth's dynamics. The uncertainties about the future behavior of the AMOC in the 21<sup>st</sup> century due to the short period of *in situ* observations bring into discussion divergent statements about the effects in the thermohaline circulation. In addition, despite of some divergences, the future predictions based on model results still bring into evidence the

consequences that such physical impacts and hence the impacts on climate might have on societies.

**Figure 3** - AMOC circulation emphasizing the transport through the Atlantic basin and reaching both sites of North Atlantic Deep Water (NADW) production (BEAL et al., 2011)



Source: BEAL et al., 2011.

Paleoclimatic and paleoceanographic studies provide data required to calibrate these model predictions making climate models progressively more reliable, being a powerful tool to calibrate and try to measure the magnitude of the future climate impacts on Earth's system. Different environmental compartments and dynamics are considered to construct future models like the atmosphere, vegetation, and mainly oceanic behavior and variability.

The AMOC plays a vital role in the inter-hemispheric connection and is responsible for the distribution of salt and heat from low latitudes and tropical regions to high latitudes in the Northern Hemisphere. Its dynamics is fundamental to the establishment of the Earth's climate and due to the large thermal property and heat distribution capacity of the oceans, acting as climate modulators. Past changes in AMOC intensity were responsible for significant changes in ocean water properties (BARD, 2000) as well as influencing the atmosphere and hence the climate on the continent (MULITZA et al., 2008).

Covering different aspects, the fragility of the climate system has been emphasized in AMOC studies, and the conclusions are, if not alarming, at least worrisome. For example in the North Hemisphere, Hansen et al. (2001) present a 20% reduction in the overflow of deep waters through the Greenland–Scotland Ridge that feeds the densest portion of the AMOC on the northern Atlantic, crucial for a stable conveyor of the thermohaline circulation. Bryden et

al. (2005) show that the strength of the AMOC has decreased by more than 30% over the last five decades. Other paleoclimatic records suggest that past shutdowns of the AMOC triggered ice ages with dramatic decreases of the temperatures in western Europe. In contrast, studies in South Atlantic reveal that temperature and salinity have been increasing in recent decades into the tropical Atlantic region and in South Atlantic Subtropical Gyre (STG) (WEN; CHANG; SARAVANAN, 2010). These changes in the heat content in the past or the present alter the physical, chemical and biological properties, modifying the water masses geometry and, consequently, the ocean circulation patterns and, nowadays, these effects have been interpreted as evidence of climate change. In this sense, studies covering the modes and ocean variability patterns on a millennial-scale and large temporal series are fundamental to understand the current climate and to calibrate future climate models (BARKER et al., 2009; CLARK et al., 2002; RAHMSTORF, 2002; RITZ et al., 2013).

Studies approaching the AMOC variability show that the Last Interglacial (MIS 5e) can be considered as one of the best past analogs of the current interglacial conditions, without interference from any impact of anthropic origin (MCMANUS et al., 1994). Thus, studies related to this period are essential for understanding the feedback patterns and especially the potential climatic impacts resulting from oceanographic changes. In addition, the absence of studies in the western South Atlantic in a high resolution covering the Last Interglacial represents a limitation in the use of paleocirculation data from analog periods through their comparison to the current climate, and to calibrate future climatic projections.

In this sense, we used the core GL-1090 with focus on the interval between 110-140 ka, exploring the evolution of thermocline temperature and salinity in the Santos Basin during Termination II and the Last Interglacial. The dissertation is divided into five main chapters: Chapter 1 explores the applicability of paleoceanographic researches to society and contextualizes the dissertation theme; Chapter 2 presents the main objectives covered in this work; Chapter 3 is dedicated to building up a theoretical basis based on the literature, covering the main topics related to our research; Chapter 4 approaches our discussion, the chapter content is the submitted manuscript under revision in the *Paleoceanography and Paleoclimatology* journal; and Chapter 5 deals with our general conclusions and future perspectives about our interpretations. In summary, our results suggest that to an efficient transport toward the North Hemisphere and, thus AMOC recovery in an interglacial mode during the Last Interglacial, an accumulation of salt and heat from the Agulhas Leakage waters in the South Atlantic subtropical gyre is needed before being released in two-phases northward and feed the two sites of North Atlantic Deep Water production. The mechanism

proposed approximates the Agulhas Leakage intensification and the two-phase AMOC recovery during the Last Interglacial, in which a favorable ocean-atmospheric configuration is needed to release the salty anomalies across the Equator. We believe that the results presented here will be beneficial for paleoclimatologists and climate modelers, allowing further understanding the role of the tropical South Atlantic as a source of density that forces the AMOC and influences the global climate.

## 2 OBJECTIVES

The study aims to reconstruct the conditions of the thermocline evolution in the western subtropical South Atlantic during Termination II and the Last Interglacial. Additionally, into this topic the following themes will be explored:

- Which forcing has greater influence on the  $\delta^{18}\text{O}$  of *G. inflata* (thermocline layers), and leads the isotopic shift to an interglacial configuration during part of MIS 5e.
- The extension of Agulhas Leakage waters influences into the western South Atlantic during the Termination II and the beginning of the Last Interglacial.
- The timing and mechanisms responsible for the AMOC recovery during the Last Interglacial.
- A plausible mechanism evolving ocean-atmosphere gateway controlling the northward transmission of buoyancy anomalies from tropical regions in the South Atlantic.

### 3 LITERATURE REVIEW

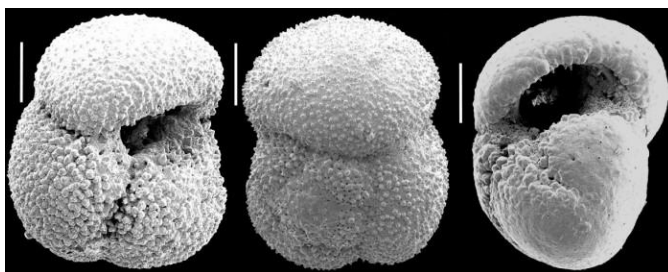
#### 3.1 THE USE OF PLANKTIC FORAMINIFERA APPLIED TO PALEOTEMPERATURE AND SALINITY RECONSTRUCTIONS

This topic provides supporting information about the main geochemical proxy employed in this work and concerning geochemical analysis, and it was applied in the planktic foraminifer *Globorotalia inflata*.

The distribution of planktic foraminiferal species in the ocean tends to correlate with temperature and the calcitic mineralogy of their tests make them an attractive group for geochemical analyses that has been widely used in paleoceanographic studies (KATZ et al., 2010). However, due to the substantial physical and chemical gradients existent in the upper water column, knowledge of a species preferred depth habitat and/or seasonal biases is required to make more accurate interpretations of geochemical data. In addition, the stable isotopic composition of planktic foraminifera is frequently used as a tool for monitoring temporal variations in the vertical structure of the upper ocean (CLÉROUX et al., 2007; MULITZA et al., 1999; SPERO et al., 2003).

*Globorotalia inflata* (Figure 4) is the main species used in this work due to its vertical distribution in the water column. It is the most abundant deep-dwelling transitional water species in the South Atlantic, established between subtropical and polar water masses encompassing the Subtropical Front (STF) and Subantarctic Front (SAF) in thermocline layers of the ocean (GROENEVELD; CHIESSI, 2011).

**Figure 4** - The main foraminifera specie employed in this study: *Globorotalia inflata* (250-300  $\mu\text{m}$ )



##### 3.1.1 Stable oxygen isotope ( $\delta^{18}\text{O}$ ) applied in paleoceanographic studies

The stable isotope ratios applied in planktic and benthic foraminifera are the most traditional and widely used proxy in paleoceanography studies as the isotope compositions



from their tests have a relationship with water column properties (KATZ et al., 2010; STEPH et al., 2009). In the  $^{18}\text{O}/^{16}\text{O}$  ( $\delta^{18}\text{O}$ ) ratio is dependent upon the temperature during the calcification process,  $\delta^{18}\text{O}$  from seawater ( $\delta^{18}\text{O}_{\text{sw}}$ , commonly used as a salinity proxy) and particularly on the amount of ice stored in continental ice-sheets at the poles. Emiliani (1955) found a periodic variation in the ratio of  $^{18}\text{O}/^{16}\text{O}$  analyzing tests of planktic foraminifera from several marine sediment cores and interpreted these oscillations as related to glacial-interglacial changes. Working on sediments sampled with long piston cores, Emiliani showed using  $\delta^{18}\text{O}$  that there had been many more at least eight glaciations during the late Pleistocene and the tropical temperature would have varied between 6 – 8 °C (EMILIANI, 1966). These advances were crucial to establishing the isotope stage stratigraphy system; today commonly referred as Marine Isotope Stages (MIS) (BASSINOT, 2007).  $\delta^{18}\text{O}$  variations found in marine sediments are thus related to climate, and the variation through time is dominated by cycles that can be correlated with the orbital variations in solar radiation (ANDERSON, 2007).

This good relationship with environmental conditions is because of the fractionation due to different processes that occur in nature. The fractionation during evaporation produces  $^{16}\text{O}$  enriched precipitation over land, result in  $^{16}\text{O}$  enriched glacial ice sequestered on land and  $^{16}\text{O}$  enriched river runoff to the oceans. In general, in a long time-scale perspective,  $^{18}\text{O}$  enriched values of carbonate  $\delta^{18}\text{O}$  are observed through glacial climate, in which a larger fraction of  $^{16}\text{O}$ -enriched snow and ice persists through cooler summers and accumulates into large continental ice sheets. The opposite is expected during warmer periods in which most high-latitude precipitation returns to the oceans via summer ice and snow melt a non-enriched  $\delta^{18}\text{O}$  concentrates in the ocean (KATZ et al., 2010; STEPH et al., 2009). The  $\delta^{18}\text{O}$  is the first geochemical proxy commonly applied in foraminiferal tests, remaining as a crucial tool for paleoceanography reconstructions and used as a paleothermometer, ice-volume, and sea-level indicator, thus as a correlation tool.

### **3.1.2 Magnesium to calcium ratio (Mg/Ca) and derived oxygen isotope of seawater ( $\delta^{18}\text{O}_{\text{sw}}$ )**

Mg/Ca has been commonly used as a powerful proxy to reconstruct marine paleotemperatures (ANAND; ELDERFIELD; CONTE, 2003; DEKENS et al., 2002; LEA; MASHIOTTA; SPERO, 1999). The ratio of magnesium to calcium is nearly constant throughout the ocean, and the residence time for both elements is longer than a million years, and as main advantage over other marine paleothermometry proxies is that the temperature

estimated can be obtained from the same biotic carrier from which oxygen isotopes  $\delta^{18}\text{O}$  are obtained (SCHMIDT; SPERO; LEA, 2004). This ratio concentration has a direct relationship with temperature due to the substitution of  $\text{Mg}^{2+}$  into marine calcites being favored at higher temperatures (LEA; MASHIOTTA; SPERO, 1999). Different calibrations of this relationship are expressed as equations and have been applied successfully to the paleorecords in a wide range of time periods (ANAND; ELDERFIELD; CONTE, 2003; CLÉROUX et al., 2008, 2013b; GROENEVELD; CHIESSI, 2011; LEA; MASHIOTTA; SPERO, 1999). In addition, paired Mg/Ca concentrations and  $\delta^{18}\text{O}$  from calcite measurements on planktic foraminifera are often used to reconstruct  $\delta^{18}\text{O}_{\text{sw}}$ , a robust proxy for salinity that could be affected by evaporation and precipitation, among other hydrological effects and in a glacial-interglacial variability also depends on global changes in ice volume (CLÉROUX et al., 2008). Therefore, Mg/Ca ratios coupled with  $\delta^{18}\text{O}_{\text{sw}}$  can ensure a common source of the signal, averaging the same environmental conditions, season and spatial habitat, minimizing errors and uncertainties for these water column reconstructions.

### 3.2 THE ROLE OF AGULHAS LEAKAGE ON GLACIAL TERMINATIONS

The Atlantic meridional overturning circulation plays a key role in the global climate system. It consists of northward transport of warm and salty near-surface waters from the tropical Atlantic to both sites of North Atlantic Deep Water (NADW) formation in the Labrador and Nordic seas, becoming dense and sinking, then flowing southward as a return flow at depth (BUIZERT; SCHMITTNER, 2015). Perturbations to the AMOC strength were observed in previous records from the glacial period that present a significant slowdown of its flow linked to fresh water discharges from North Atlantic melting ice sheets (e. g. (CLARK et al., 2002; McMANUS et al., 2004), causing instabilities in the density gradient of the northern ocean.

The slowdown of AMOC modulating its different modes (BÖHM et al., 2015), has been suggested as a cause of climate change due to the weakening of northward heat transport from the southern ocean to the high latitudes (CROWLEY, 1992). These variabilities are expected in glacial Terminations (glacial-interglacial transition) and impact both hemispheres



climatically oppositely, known as a bipolar seesaw effect (BROECKER, 1998; CROWLEY, 1992; STOCKER; JOHNSEN, 2003).

Paleoceanographic proxies provide evidences for a surface cooling and freshening at both sites of deep water formation in the northern hemisphere during glacial periods concomitant to sea surface salinity (SSS) increase in the western tropical/subtropical Atlantic (CARLSON et al., 2008; SCHMIDT; SPERO; LEA, 2004; WELDEAB; SCHNEIDER; KÖLLING, 2006). In this sense, the primary source of heat and salty waters to the subtropical South Atlantic is from the Indian Ocean via the Agulhas Leakage (AL) waters. The AL is a major component of the AMOC, in which is responsible for transporting AL waters towards the subpolar North Atlantic as the upper limb of the meridional circulation to the northern hemisphere (Figure 5) (BIASTOCH; BÖNING; LUTJEHARMS, 2008; MOROS et al., 2002). The AL provides a vital source of negative buoyancy that forces the AMOC (BIASTOCH; BÖNING; LUTJEHARMS, 2008; BUIZERT; SCHMITTNER, 2015). Therefore, Indian–Atlantic exchange of heat and salt plays a role in maintaining the high surface salinity, the strength and stability of northern sinking circulation (WEIJER, 2002; WEIJER; DE RUIJTER; DIJKSTRA, 2001).

Nowadays, the AL is the result of a complex and non-linear interplay between the strong western boundary current (Agulhas Current) along the South Africa Coast and the separation point where part of the Agulhas waters retroflect back to the Indian Ocean (BIASTOCH et al., 2009b; LUTJEHARMS, 2006). The retroflection process is linked to the formation of edges and filaments (Agulhas rings) through instabilities where part of these waters invade the South Atlantic carrying warm and salty surface and intermediate waters that are being incorporated into the subtropical gyre (DE RUIJTER et al., 1999). The bulk of the AL and the rings path northward through the South Atlantic happens below the surface at the depths of the thermocline (DOGLIOLI et al., 2006; DONNERS; DRIJFHOUT, 2004; VAN

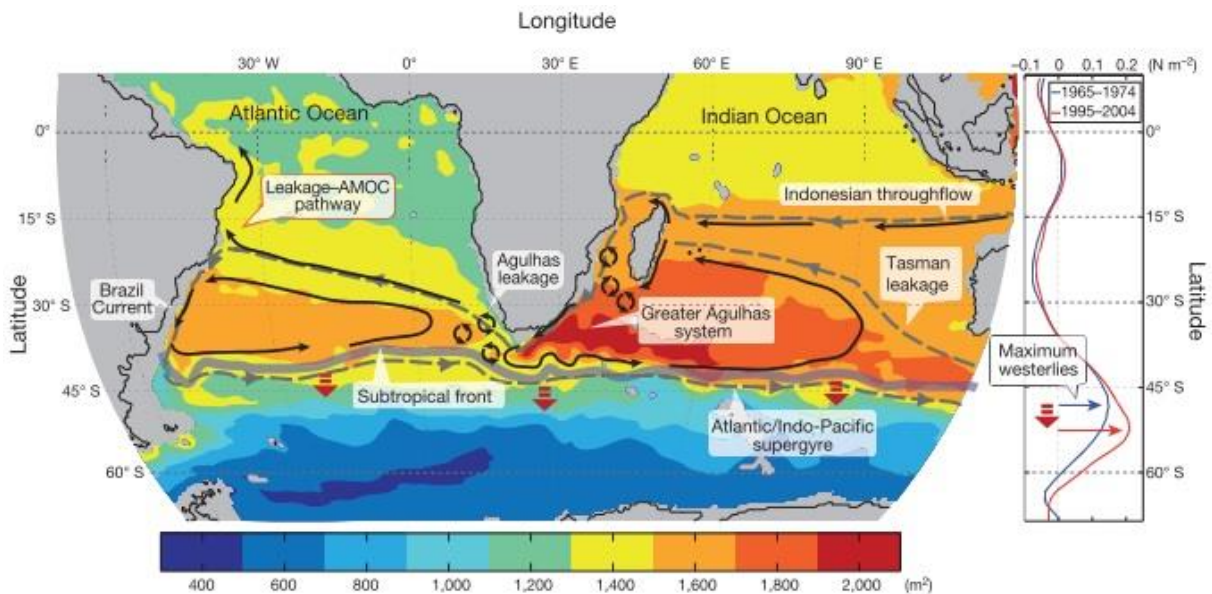
SEBILLE et al., 2010) being mainly incorporated by South Atlantic Central Waters (SACW) (GORDON et al., 1992). During its path the anomalies of more than  $\sim 1.5$  Sv emerge near latitude  $30^{\circ}\text{S}$  and rapidly propagate toward equator (BIASTOCH; BÖNING; LUTJEHARMS, 2008) as previous ocean model studies (GETZLAFF, 2005; JOHNSON; MARSHALL, 2002) and climate models (DONG; SUTTON, 2002) describe as Kelvin and Rossby wave processes. These waves can transport energy over an entire basin or even between hemispheres (JOHNSON; MARSHALL, 2002), being faster than it would be by advective transport of energy (GARZOLI et al., 1999).

A significant change in this inter-ocean exchange has also been reported over the geological period in both millennial and orbital time-scales (DYEZ; ZAHN; HALL, 2014; MARINO et al., 2013; PEETERS et al., 2004). Peeters et al. (2004) found relatively low contributions of “Agulhas Leakage fauna” in the Cape Basin, suggesting a reduced AL during glacial stages coinciding with low sea surface temperatures (SSTs), emphasizing a restriction in the AL during cold periods. In summary, during full glacial periods, the AL presents less leakage than interglacial stages, and greater intensification was a persistent feature during glacial terminations (CALEY et al., 2012, 2014; PEETERS et al., 2004). This intensification also results of a deglacial reorganization of the Southern Hemisphere westerlies (TOGGWEILER; RUSSELL; CARSON, 2006) due to their southern shift (BIASTOCH et al., 2009b; BIASTOCH; BÖNING, 2013; SIJP; ENGLAND, 2009). Sea surface temperature and salinity reconstructions inferred that AL variability is a consequence of changes in wind fields related to a southward position of the subtropical front and Antarctica ice masses (BARD; RICKABY, 2009; KASPER et al., 2014a). During glacial terminations, the sea surface temperature in the region of the leakage leads global ice-volume decrease by several thousand years (CORTESE; ABELMANN; GERSONDE, 2007). The hypothesis that peak AL occurred during glacial terminations and plausibly conduce the AMOC to shift to its full-

strength interglacial mode (KNORR; LOHMANN, 2007; PEETERS et al., 2004), in which during Termination II is observed the most prominent intensification of AL volume into South Atlantic over the past 640 ky (CALEY et al., 2014).

In that manner, AL can affect AMOC in two ways, firstly, in a mesoscale activity the influence of these waters induces wave processes in the South Atlantic that dynamically modulate the AMOC on decadal timescales (BIASTOCH; BÖNING; LUTJEHARMS, 2008); secondly in a longer timescale, the northward advection of salinity anomalies influences deep-water formation in the North Atlantic (WEIJER, 2002). These evidences give support to the idea that salinity and temperature oscillations across this ocean gateway are a fundamental factor to alter the upper northern Atlantic buoyancy and to return the AMOC to its interglacial mode (BEAL et al., 2011). In this sense, the Indian-Atlantic ocean exchange forms a critical link in climate change and precondition deglaciation processes (PEETERS et al., 2004).

**Figure 5** - Schematic representation of the Agulhas system and invasion of Agulhas waters into the South Atlantic. Position of subtropical front and emphasis on the intensification of westerly winds as a oceanic gateway mechanism leading the Indian-Atlantic connection (BEAL et al., 2011).



Source: BEAL et al., 2011.

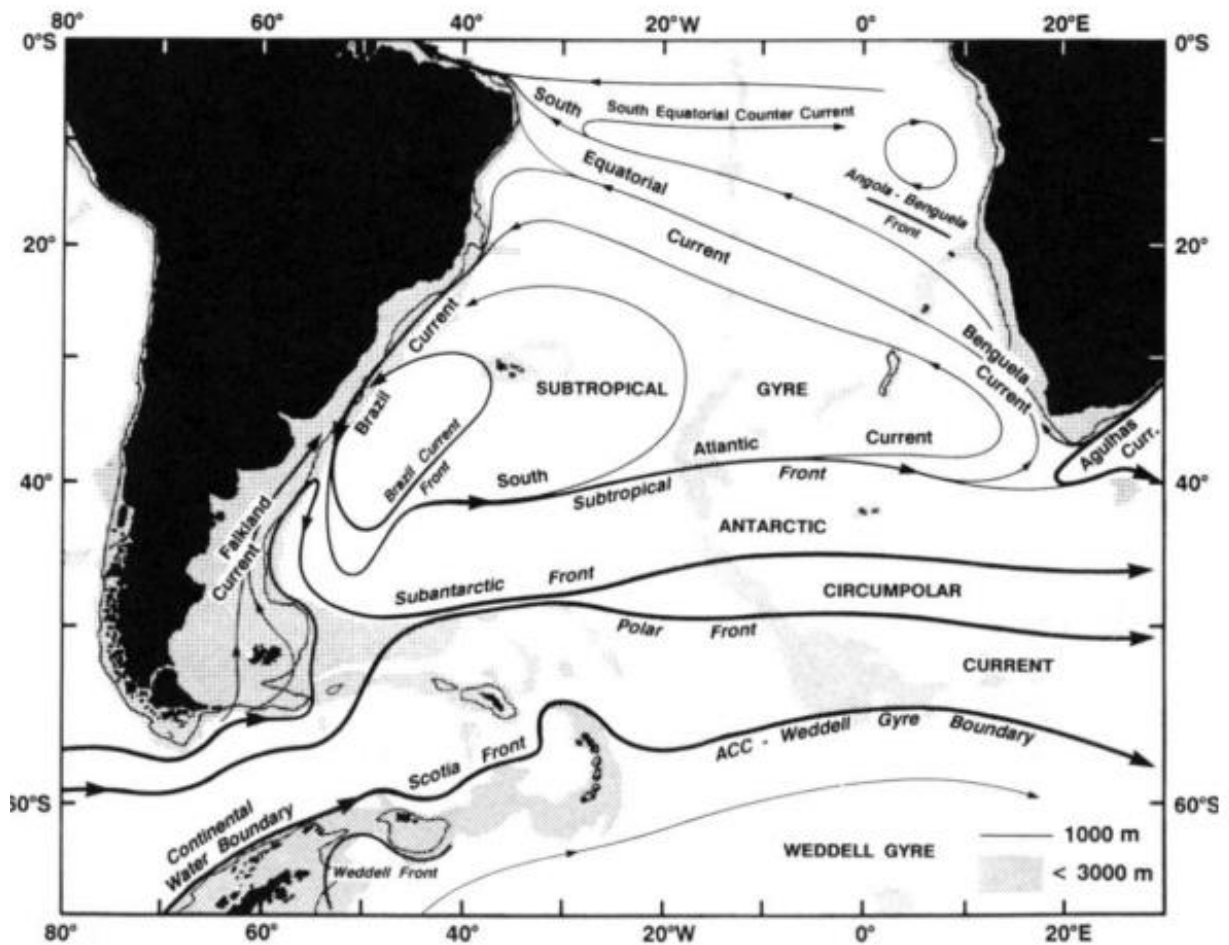
### 3.3 THE SOUTH ATLANTIC SUBTROPICAL GYRE

Subtropical gyres are the oceanic response of the wind-driven circulation pattern effect at mid-latitudes. The principal feature is the transport of water from these regions toward equator and high latitudes, playing a crucial role modulating the global climate variability. The STG is the main component of the superficial circulation dynamics of the South Atlantic ocean and fills a significant part of its basin (PETERSON; STRAMMA, 1991). It encompasses a system of wind-driven surface currents flowing anti-clockwise (anti-cyclonic) and is composed by the southward-flowing western boundary Brazil Current (BC), which flows along the South American coast until 33-38°S, meeting the northeastward extension of the Antarctic Circumpolar Current (ACC) into the Atlantic, the Malvinas Current, considered as the most energetic region in the southern Atlantic Ocean known as the Brazil-Malvinas Confluence (GARZOLI, 1993; GORDON, 1985, 1989). From this point, the eastward flow is established and originates the South Atlantic Current (SAC), the southern boundary of the STG (OLSON et al., 1988; PETERSON; STRAMMA, 1991b; SILVEIRA et al., 2000). The SAC encounters the Benguela Current (BeC) flowing northward, along the African continent, where it turns into the southern branch of the South Equatorial Current (SEC), the current that forms the northern edge of the subtropical gyre (GONI; BRINGAS; DINEZIO, 2011; PETERSON; STRAMMA, 1991). The SEC bifurcation around 10°S originates two western boundary currents, represented by BC and its northward flow, crossing the equator, the North Brazil Current (NBC) (SILVEIRA et al., 2000).

The BC and NBC play a key role in the transfer of energy between the southern and northern hemispheres (PETERSON; STRAMMA, 1991b), as well as between the ocean and the atmosphere (CRONIN et al., 2010). In that sense, SEC bifurcation determines if the upper ocean layers become part of the AMOC continuous northward flow to the North Hemisphere or they recirculate in the South Atlantic subtropical gyre, favoring NBC or BC transport respectively (MARCELLO; WAINER; RODRIGUES, 2018). This energy partition between the northward and the southward branch of the South Atlantic western boundary currents has a vital role in the communication of the signal between southern and northern Atlantic and thus modulate the AMOC intensity (GARZOLI et al., 2013). In summary, STG acts as a conduit for the warm and saline upper waters across the equator (GARZOLI; MATANO, 2011; GORDON, 1986), where these waters are mainly fed by the Agulhas Leakage waters from the subtropical Indian Ocean, increasing heat and salinity into South Atlantic (Figure 6) (BEAL et al., 2011; BIASTOCH et al., 2009a; GORDON et al., 1992).

Throughout AL path into the STG, the air-sea surface interactions modify the signal through processes like evaporation and convection, strengthening the salt anomaly related to AL (WEIJER, 2002), turning the South Atlantic relatively warmer and saltier through thermocline layers in comparison with other sources (BYRNE; GORDON; HAXBY, 1995). These processes would be responsible for different trajectories comparing surface and sub-surface layers (RICHARDSON, 2007) with a significant impact on the transport of salt and heat anomalies throughout the Atlantic basin. This behavior may have a great influence on the STG hence over AMOC vigor, but there are still uncertainties about the role of the South Atlantic in the inter-hemisphere connections, based on the fact that the South Atlantic is not just a passive conduit for water masses, but actively influences them through air-sea interactions, mixing, and subduction and advection processes (GARZOLI; MATANO, 2011).

**Figure 6** - Schematic example of surface currents in the tropical South Atlantic (from PETERSON; STRAMMA, 1991).



Source: PETERSON; STRAMMA, 1991.

## 4 DISCUSSION

As mentioned in the General Introduction (see section 1), in this work Chapter 4 corresponds to the manuscript in revision in the *Paleoceanography and Paleoclimatology journal*.

### 4.1 LAST INTERGLACIAL INTER-HEMISPHERIC TRANSMISSION OF AGULHAS LEAKAGE CONTROLLED BY THE WESTERN SOUTH ATLANTIC<sup>1</sup>

#### 4.1.1 Introduction

The Atlantic meridional overturning circulation (AMOC) is a key feature of the global climate system characterized by a northward upper-ocean transport of warm and saline waters (CUNNINGHAM et al., 2007). In the high latitudes of the North Atlantic, these waters lose heat to the atmosphere, sink and flow southward carrying cold and saline waters to the Southern Ocean (KUHLEBRODT et al., 2007). In order to balance such deep-water export, an Indian-South Atlantic Ocean exchange of around 15 Sv is required (GORDON, 1985). This constitutes a central component of the meridional circulation and takes place via the Agulhas Leakage (AL) (GORDON, 1985). The saline waters of the AL is a major source of negative buoyancy to the AMOC, and its waters are carried towards the subpolar North Atlantic as the upper limb of the meridional circulation to maintain the salinity, strength and stability of deep-water convection (WEIJER et al., 2001; BIASTOCH et al., 2008; VAN SEBILLE et al., 2015).

The AL enters the South Atlantic mainly as thermocline waters (DOGLIOLI et al., 2006; VAN SEBILLE et al., 2010) by the spreading of rings and filaments which become incorporated into the South Atlantic Central Water (DE RUIJTER et al., 1999). This water mass fills most of the South Atlantic between 100 and 600 m water depth (PETERSON; STRAMMA, 1991b). Once in the South Atlantic, convection and air-sea interaction modify the AL signal strengthening its positive salt anomaly as it is advected westwards (WEIJER, 2002). This leaves the South Atlantic thermocline saltier in areas influenced by the AL compared to areas not influenced by the AL (BYRNE; GORDON; HAXBY, 1995).

---

<sup>1</sup> BALLALAI, J. M.; SANTOS, T. P.; LESSA, D. O.; VENANCIO, I. M.; CHIESSI, C. M.; JOHNSTONE, J. H.; KUHNERT, H.; CLAUDIO, M. R.; TOLEDO, F.; COSTA, K. B.; ALBUQUERQUE, A. L. S. Last Interglacial inter-hemispheric transmission of Agulhas Leakage controlled by the western South Atlantic. *Paleoceanography and paleoclimatology*, in revision.

Eventually, the AL signal propagates into the Northern Hemisphere via Kelvin waves generated along the western boundary of the Atlantic Ocean (BIASTOCH; BÖNING; LUTJEHARMS, 2008). This suggests that the western margin of the South Atlantic and both the Brazil Current (BC) and North Brazil Current (NBC) have important roles in the rapid inter-hemispheric transmission of AL signals. It also suggests that the region off Brazil may accurately record the timing of changes in the overturning circulation associated with changes in the AL (WEIJER, 2002; VAN SEBILLE & VAN LEEUWEN, 2007). As the partition of salt and heat between the BC and NBC depends on the position of the South Equatorial Current (SEC) bifurcation (MARCELLO; WAINER; RODRIGUES, 2018), the latitude where the SEC bifurcation is placed can be seen as a type of ocean gateway. This gateway controls how much subtropical water (in part composed of eastern South Atlantic AL waters) flows northward across the equator via the NBC and how much is recirculated into the subtropical gyre via the BC (MARCELLO; WAINER; RODRIGUES, 2018).

Sea surface temperature (SST) and sea surface salinity reconstructions suggest that the AL was reduced during glacial stages because of the northward position of the subtropical front in response to the expansion of Antarctica sea-ice (BARD; RICKABY, 2009; KASPER et al., 2014). During glacial Terminations, the AL volume increased rapidly and led the global ice-volume decrease by several thousand years (PEETERS et al., 2004; CORTESE et al., 2007; THIBAUT CALEY et al., 2014). This suggests that salt and heat oscillations across the Indian-South Atlantic exchange is a fundamental factor influencing the buoyancy of upper North Atlantic waters after a glacial maximum and consequently plays a key role in returning the AMOC to its interglacial mode (BEAL et al., 2011; CALEY et al., 2012). However, this hypothesis is unsettled by two main issues: (i) the scarcity of marine records that capture the downstream progression of the AL signal; and (ii) the large temporal difference between AL strengthening and AMOC resumption. For example, during the transition from the penultimate glacial (Marine Isotope Stage 6 – MIS 6) to the Last Interglacial (MIS 5e), a period known as Termination II (TII), Mg/Ca-SST and ice-volume free seawater  $\delta^{18}\text{O}$  ( $\delta^{18}\text{O}_{\text{IVF-SW}}$ , a proxy for salinity) from the eastern South Atlantic suggest an AL intensification starting already at ca. 142 ka BP (SCUSSOLINI et al., 2015). However, part of deep-water convection in the high latitudes of the North Atlantic did not recover until the late TII at ca. 129 ka BP (DEANEY; BARKER; FLIERDT, 2017). This ~ 13 ka interval suggests that AL waters were not directly transported to the regions of deep-water formation and, therefore,

other ocean gateways played a fundamental role in connecting the South to the North Atlantic and reestablish the AMOC.

Here, we present a combination of new and published Mg/Ca-SST and  $\delta^{18}\text{O}_{\text{IVF-SW}}$  data from the upper (surface and thermocline) western South Atlantic (Santos Basin, core GL-1090, 24.92 °S, 42.51 °W, 2225 m water depth). The comparison of these data with previous studies from the Walvis Ridge (eastern South Atlantic) (SCUSSOLINI et al., 2015) suggests a coherent increase in the subtropical South Atlantic salinity coeval with AL strengthening during TII and early-MIS 5e. During MIS 5e, our results show a two-phase abrupt freshening of the western margin in the surface at ca. 129 ka BP and thermocline at ca. 124 ka BP. This resembles the two-phase resumption of the AMOC during the Last Interglacial (DEANEY; BARKER; FLIERDT, 2017) and suggests that AL dense waters accumulated in the South Atlantic subtropical gyre were released by the western boundary to the North Atlantic in two pulses during early- and mid-MIS 5e. We propose a mechanism where not only a strong AL is needed to return the AMOC to its interglacial mode but also a favorable ocean-atmosphere configuration that allows the AL signal to reach the Northern Hemisphere. Our results, therefore, connect AL to the sites of deep-water formation in the high latitudes of the North Atlantic during glacial-interglacial transitions.

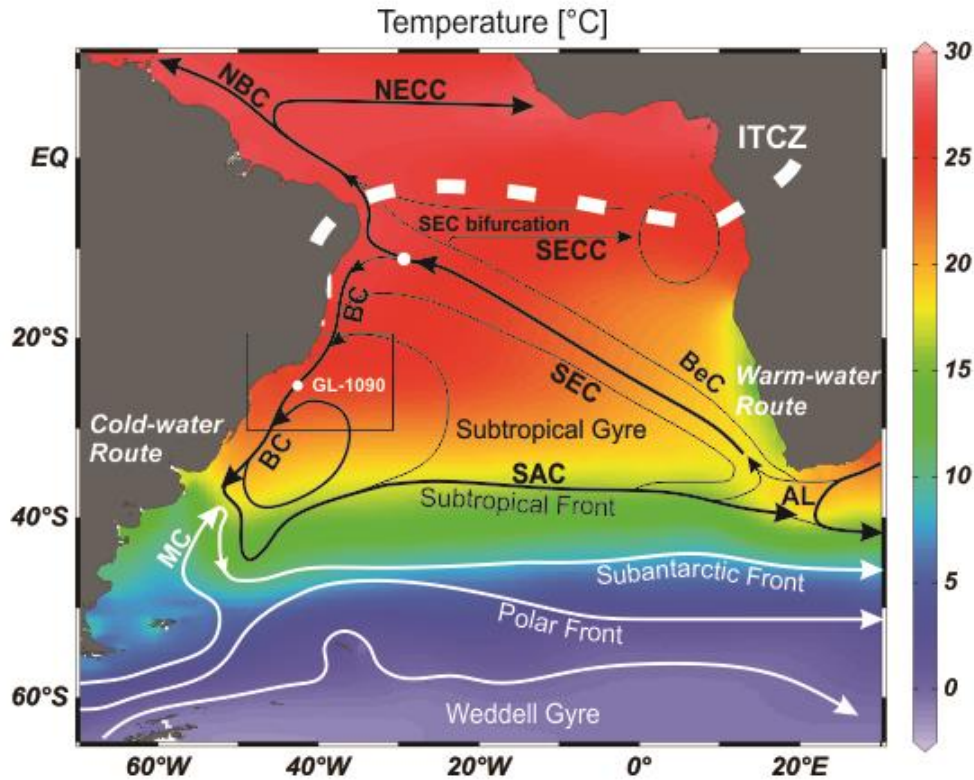
#### 4.1.2 Study Area

Core GL-1090 was collected in the Santos Basin, (western South Atlantic, 24.92°S, 42.51°W, 2225 m water depth – Figure 7). The upper ocean circulation in this region is controlled by the Brazil Current (BC), which is the western boundary current of the South Atlantic subtropical gyre. The BC originates at ca. 10 °S from the southern branch of the bifurcation of the South Equatorial Current that is also the source of the northward-flowing North Brazil Current (PETERSON; STRAMMA, 1991b). The BC shows its highest intensity during austral spring and summer when the Intertropical Convergence Zone (ITCZ) shifts southward and the northeasterly trade-winds are stronger (RODRIGUES; ROTHSTEIN; WIMBUSH, 2007). At the surface, the BC transports the Tropical Water characterized by warm ( $> 20$  °C) and salty ( $> 36$ ) waters formed by the high incoming solar radiation and excess of evaporation of the tropical South Atlantic (STRAMMA; ENGLAND, 1999). Around 38 °S, the BC collides with the northward-flowing Malvinas Current, producing the Brazil–Malvinas Confluence. In this region and locations between the Argentine basin and the mid-Atlantic ridge, thermocline water is generated by air-sea interaction (GARZOLI;



MATANO, 2011). These waters recirculate within the South Atlantic subtropical gyre and are transported southward by the BC below the Tropical Water between ca. 100 – 600 m. The waters in the thermocline are generally referred to as South Atlantic Central Water (SACW), which is colder ( $\sim 6 - 20$  °C) and fresher (34.5–36.2) compared with the surface Tropical Water (PETERSON; STRAMMA, 1991b). SACW is also sourced from Indian Ocean Central Water and brought into the eastern South Atlantic by the leakage of waters of the Agulhas Current in the upper 1000 m of the water column (GORDON et al., 1992). The Agulhas Current carries thermocline waters from the South Indian Ocean subtropical gyre with contributions from the Red and Arabian seas, the Indonesian throughflow and the equatorial Indian Ocean via eddies and meanders of the Mozambique Channel and the East Madagascar Current (SONG et al., 2004; BEAL et al., 2006; LUTJEHARMS, 2006). The Agulhas Current flows to the southwest along the east coast of South Africa until it separates from the continent, driven by the anticyclonic wind field over the South Indian Ocean (SONG et al., 2004; BEAL et al., 2006). This effect feeds backward water into the Indian Ocean, creating the Agulhas Retroflection. The migration of eddies and meanders of the Mozambique Channel and the East Madagascar Current downstream, associated with the bathymetry and morphology of the continental margin, destabilize the retroflection (BRYDEN et al., 2005; BIASTOCH et al., 2009). This destabilization promotes the leakage of Indo-Pacific waters into the Atlantic through rings, eddies and filaments mainly at the depths of the thermocline (GORDON et al., 1992; VAN AKEN et al., 2003; DOGLIOLI et al., 2006). In a wider context, the Agulhas system and the southern Indian Ocean subtropical gyre are embedded in a Southern Hemisphere supergyre that connects the Atlantic, Indian and Pacific basins (RIDGWAY; DUNN, 2007). Therefore, the Brazil-Malvinas Confluence (and adjacent areas) and Agulhas Leakage represent the major areas of formation of SACW and are crucial for ventilating the South Atlantic thermocline (GORDON, 1981).

**Figure 7** - Map of the South Atlantic surface circulation (modified from Peterson and Stramma, 1991) showing the spatial distribution of sea surface temperature (SST) and the position of core GL-1090. Thick black lines represent the main surface currents in South Atlantic. AL: Agulhas Leakage, BC: Brazil Current, MC: Malvina Current, NBC: North Brazil Current, SAC: South Atlantic Current, SEC: South Equatorial Current and SECC: South Equatorial Countercurrent. Dashed white line shows the austral summer mean position of Intertropical Convergence Zone (ITCZ).



Source: Developed by the author, 2019.

### 4.1.3 Material and Methods

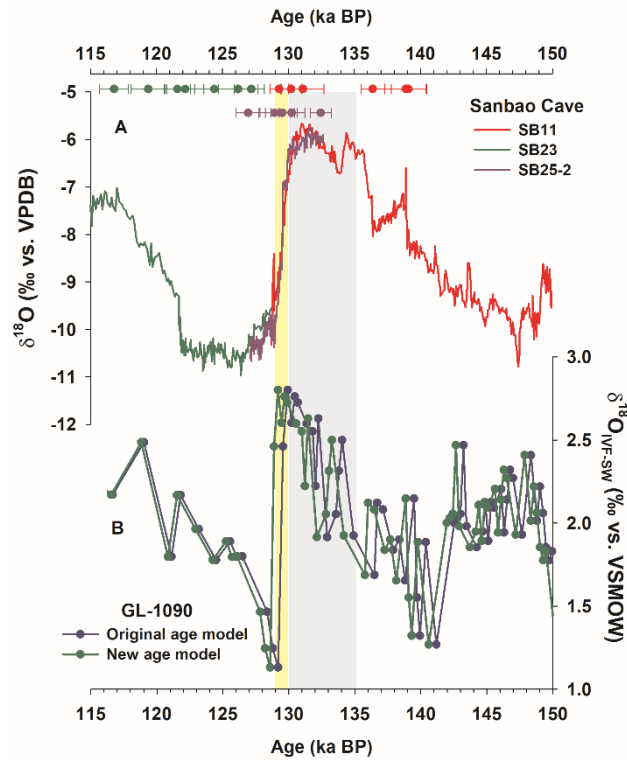
#### 4.1.3.1 GL-1090 Sampling

Core GL-1090 was collected by the Petrobras oil company in the western South Atlantic (24.92 °S, 42.51 °W, 2225 m water depth, 1914 cm long) and was sampled at approximately 2 cm resolution (SANTOS et al., 2017a). From each sample, 10 cm<sup>3</sup> of sediment was wet-sieved over a 150-μm mesh and the residual material was oven-dried for 24 h at 50 °C. The dried material was handpicked with a stereomicroscope to select ideal shells of planktic foraminifera *Globorotalia inflata* (Figure 4), a thermocline dweller planktic foraminifera to the Mg/Ca analysis described below (see section 4.1.3.3).

#### 4.1.3.2 Age Model

Core GL-1090 covers the last 185 ka, its Bayesian age model (BLAAUW; CHRISTEN, 2013) was obtained through a combination of calibrated AMS  $^{14}\text{C}$  ages and benthic foraminifera  $\delta^{18}\text{O}$  tie points aligned to two reference curves (LISIECKI & RAYMO, 2005; GOVIN et al., 2014). Most of the benthic  $\delta^{18}\text{O}$  tie points were obtained by the alignment of GL-1090 with MD95-2042, which has been updated to the AICC2012 ice core chronology (BAZIN et al., 2013; VERES et al., 2013; GOVIN et al., 2014). This is the most appropriate age reference to display marine and ice core records over the Last Interglacial, because of the numerous new stratigraphic links that significantly reduce dating uncertainty (CAPRON et al., 2014). In the original version of GL-1090 age model (SANTOS et al., 2017a), the abrupt decrease in the surface  $\delta^{18}\text{O}_{\text{IVF-SW}}$  of  $-1.67\text{‰}$  at the end of TII occurs between 129.9 ka BP and 129.1 ka BP (1404 and 1400 cm of core GL-1090, respectively) with a mean estimated age uncertainty of 3.87 ka. Taking into account that the mechanism discussed here, i.e., the coupling between the ITCZ wind-stress and the bifurcation of the South Equatorial Current, is the main controller of the surface salinity in the western South Atlantic, we assumed one of the radiometrically  $^{230}\text{Th}$  ages of Sanbao cave speleothem (SB11) (WANG et al., 2008) as a tie-point for the transition at end of TII (Figure 8). Wet and dry conditions in Sanbao cave are also associated with the north-south migration of the tropical rain belt represented by the ITCZ. Therefore, we align the abrupt shift of the Santos Basin surface  $\delta^{18}\text{O}_{\text{IVF-SW}}$  with the fast northward movement of the tropical rain belt represented by the ITCZ (Figure 8). In Sanbao Cave,  $\delta^{18}\text{O}$  values shifted from extremely dry conditions (ca.  $-6.9\text{‰}$ ) at 129.6 ka to a wet climate (ca.  $-10\text{‰}$ ) at 128.8 ka. The nearest  $^{230}\text{Th}$  age is located at  $129.3 \pm 0.7$  ka, which is approximately midway (ca.  $-8\text{‰}$ ) between weak and strong monsoon. Then, we removed a previous tie-point located at 1403 cm (SANTOS et al., 2017a) and aligned  $^{230}\text{Th}$  age  $129.3 \pm 0.7$  ka at 1402 cm (the midway  $\delta^{18}\text{O}_{\text{IVF-SW}}$  transition) as a new tie-point for core GL-1090. We could consider that there is a more precise  $^{230}\text{Th}$  age for this transition of  $129.0 \pm 0.1$  ka, however, the use of this age produces an uncertainty much lower (0.51 ka) than the one reported by the AICC2012 ice core chronology for the transition to the Last Interglacial (1.72 ka) (BAZIN et al., 2013), which we consider unfeasible.

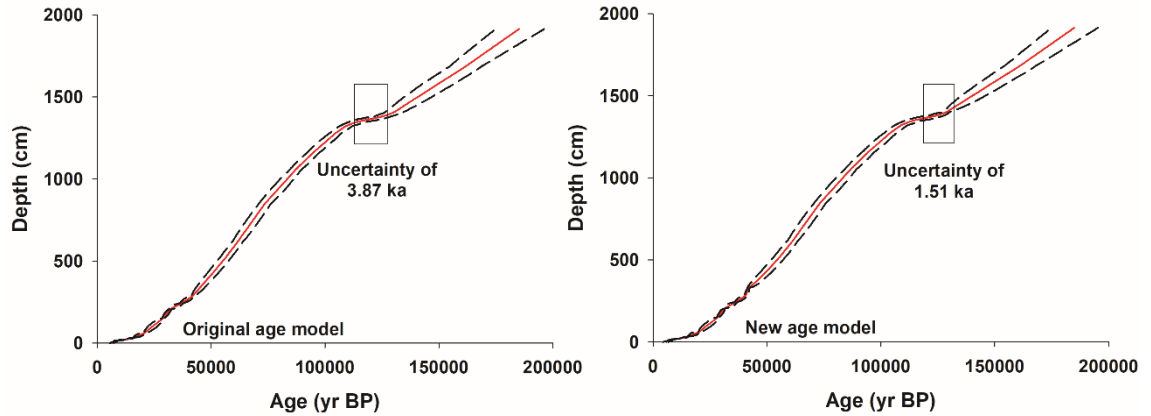
**Figure 8** - Alignment between Santos Basin surface  $\delta^{18}\text{O}_{\text{IVF-SW}}$  with records of Asian Monsoon from Sanbao Cave with their respective radiometrically  $^{230}\text{Th}$  ages (WANG et al., 2008). The new age model of core GL-1090 (green) produces slightly younger ages across the transition to the Last Interglacial compared with the previous one (blue). Grey bar highlights the weak Asian Monsoon period correspondent to Heinrich stadial 11 and yellow bar the transition to strong Asian Monsoon at the onset of the Last Interglacial.



Source: Source: Developed by the author, 2019.

The new Bayesian age model places the surface  $\delta^{18}\text{O}_{\text{IVF-SW}}$  transition between 1404 and 1400 cm at a slightly different interval between 129.1 ka BP and 128.5 ka BP, but with a significant reduction in the mean uncertainty from 3.8 ka (original age model (SANTOS et al., 2017a)) to 1.5 ka (new age model, see Figure 8 and 9). In general, the new Bayesian age model produced a final chronology ca. 140 years younger than the original run for the 1914 cm of core GL-1090. However, the update in age model did not result in significant changes in sedimentation rate, which sustain earlier interpretations based on this core (SANTOS et al., 2017a, 2017b) (Figure 9). The mean uncertainty decrease more strongly between ca. 136 and 126 ka (from Heinrich stadial 11 to the early Last Interglacial), where reductions of more than 2 kyr were attained (e.g. at 1407 cm) (Figure 9).

**Figure 9** - Comparison between original (left) (SANTOS et al., 2017a) and new (right) Bayesian age-depth model of core GL-1090. The main features of sedimentation rate were preserved but the uncertainty was significantly reduced around the period of interest for this study.



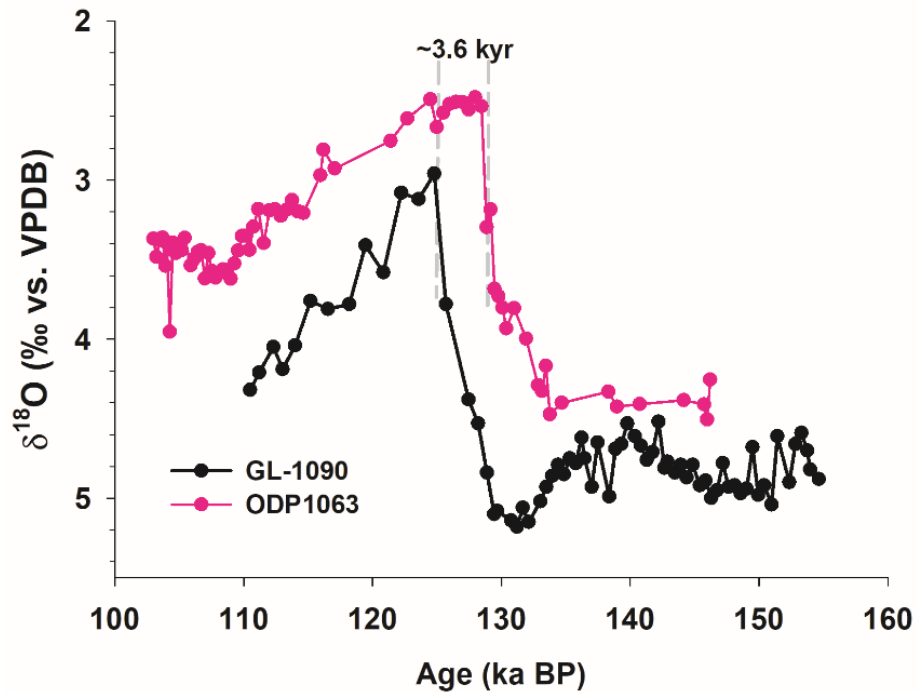
Source: Source: Developed by the author, 2019.

A similar strategy was adopted by Deaney et al. (2017) choosing the abrupt rise in  $\text{CH}_4$  at  $\sim 128.7$  ka in Antarctica ice core (LOULERGUE et al., 2008) to update the age model of core ODP1063. As this rise is attributed to the release of methane by boreal wetlands after the northward shift of the tropical rain belt, it is possible to affirm that GL-1090 and ODP1063 consider related assumptions to recalculate their age models, i.e., a fast northward migration of the ITCZ and then had similar age uncertainty of 1.51 ka and 1.72 ka, respectively, around the end of TII. Furthermore, interglacial benthic  $\delta^{18}\text{O}$  minimum of core ODP1063 initiated  $\sim 3.6$  kyr before core GL-1090 (Figure 10), which is in good agreement with studies that correlated Southern Ocean and North Atlantic Last Interglacial climate evolution (GOVIN et al., 2012).

According to Govin et al. (2012), the combined age uncertainty that needs to be considered when comparing Southern Ocean to North Atlantic records reach at most  $\pm 2$  ka over the period of 130-115 ka. Within this period, the benthic  $\delta^{18}\text{O}$  plateau starts at around 130 ka in the North Atlantic, which is 3.5 ka earlier than in the Southern Ocean. This offset likely results from the rapid transmission of  $^{18}\text{O}$ -depleted meltwater to the deep North Atlantic and/or peak northern summer insolation at early MIS 5e. On the other hand, southern regions would depend on the slower equilibration of this signal throughout deep-ocean circulation. Figure 10 shows that a similar time lag exists between benthic  $\delta^{18}\text{O}$  of core GL-1090 and ODP1063. This demonstrates that our age-depth model is consistent with the time-

frame that is usually found in other investigations that explore the lead-lag nature of deep-ocean  $\delta^{18}\text{O}$  (Govin et al., 2012 and references therein).

**Figure 10** - Comparison between benthic  $\delta^{18}\text{O}$  of cores GL-1090 (black) (SANTOS et al., 2017a) and ODP1063 (pink) (DEANEY; BARKER; FLIERDT, 2017). The shift to low  $\delta^{18}\text{O}$  during peak MIS 5e occurred approximately 3.6 kyr earlier in the North Atlantic core ODP1063.



Source: Source: Developed by the author, 2019.

#### 4.1.3.3 Calculation of thermocline temperature and ice-volume free seawater $\delta^{18}\text{O}$

Mg/Ca measurements were performed on samples comprising 9 - 30 individuals of the planktic foraminifera *Globorotalia inflata* from the 250 - 300  $\mu\text{m}$  size fraction. A plankton tow study at the central Walvis Ridge (eastern South Atlantic) suggests that the base of the calcification depth of this species is situated between 300 and 400 m in summer and winter, respectively (LONČARIĆ et al., 2006). From a transect of surface sediment samples at the Brazil-Malvinas Confluence (western South Atlantic), Chiessi et al. (2007) proposed that *G. inflata*  $\delta^{18}\text{O}$  is consistent with a calcification depth between 200 and 400 m. In the North Atlantic, *G. inflata* lives preferentially at the base of the summer thermocline, which is about 100 m north of 35 °N, but it calcifies deeper (~ 250 m) under warmer conditions south of 35 °N (CLÉROUX et al., 2007). Such slightly different depth preferences may reflect the existence of separate genotypes among the distinct ocean basins (MORARD et al., 2011).

Although it is still not possible to safely attribute these depth preferences to different genotypes, what the previously mentioned investigations illustrate is that *G. inflata* occurs over a wide range of depths, but independently of the region, exhibits its maximum abundance in the thermocline and there is very little overlap with the depth preferences of more surface-dwelling *Globigerinoides ruber*. Therefore, we assigned *G. inflata* as a thermocline-dweller species associated, in the Santos Basin, to the South Atlantic Central Water. Furthermore, *G. inflata* is relatively constant throughout core GL-1090, making it better suited to characterize thermocline temperature than other species like *Globorotalia truncatulinoides* or *Globorotalia crassaformis*.

*G. inflata* tests were gently crushed between two clean glass plates to open the chambers and cleaned according to the protocol of Barker et al. (2003). The tests underwent ultrasonic cleaning alternated by multiple washes in deionized water and ethanol to remove clay, hydrogen peroxide treatment in a boiling water bath to eliminate organic matter and a short dilute acid leaching with 0.001 M nitric acid to eliminate any adsorbed contaminants. Then, samples were dissolved in 0.075 M nitric acid. Dissolved samples, were centrifuged for 10 min to exclude insoluble residues. The diluted solutions were analyzed with an Inductively Coupled Plasma Optical Emission Spectrometer (ICP-OES)—Agilent Technologies 700 Series with Cetac ASX-520 autosampler and a micro-nebulizer at the MARUM – Center for Marine Environmental Sciences, University of Bremen, Germany. Three replicates of each sample were run and averaged. Elements were measured at the following spectral lines: Mg (279.6 nm), Ca (315.9 nm), Sr (421.6), Al (167.0 nm), Fe (238.2 nm), and Mn (257.6 nm). Calibration standards consisted of dissolution acid (0.075 M HNO<sub>3</sub>) as blank and four multielement standards between 20 and 80 ppm Ca, with Mg/Ca of 4.12 mmol/mol. Calibrations for all elements were based on linear regressions. Instrumental precision was monitored by using an in-house external standard solution, run after every five samples. Long-term relative standard deviation of the in-house standard is <2 % for Mg/Ca. A dissolved solution of commercial limestone standard ECRM 752-1 was measured every 30 – 50 samples. This solution was measured at 3.73 mmol/mol ( $\sigma = 0.01$ , 0.24%,  $n=9$ ) during the ICP-OES run which is very close to the published value of 3.75 for centrifuged solution (GREAVES et al., 2005). In the time interval between 140 – 110 ka 64 samples were analyzed. Three samples had <10 ppm Ca and were rejected, as the calibration is non-linear at low Ca concentrations. Al/Ca is often used as a measure of clay contamination, which can bias Mg/Ca in the sample as clays often contain Mg. Mean Al/Ca for the interval analyzed

was 0.27 mmol/mol, which is below commonly accepted limits (0.3 – 0.5 mmol/mol) (LEA et al., 2005; KUHNERT et al., 2014). Further, there was no association between Al/Ca and Mg/Ca in these samples ( $r = 0.007$ ).

To convert *G. inflata* Mg/Ca ratios into temperature several calibrations are available (i.e. ELDERFIELD; GANSSSEN, 2000; ANAND et al., 2003; MCKENNA; PRELL, 2004; CLÉROUX et al., 2008, 2013; REGENBERG et al., 2009; GROENEVELD; CHIESSI, 2011). Ideally, the use of species-specific and regionally constrained equations will provide more accurate evaluation of Mg/Ca paleotemperature (ANAND; ELDERFIELD; CONTE, 2003). In this regard, the works of Groeneveld & Chiessi, (2011) and Cléroux et al. (2013) would offer appropriate equations, since they included South Atlantic core-tops samples in their species-specific calibrations for *G. inflata*. However, a number of factors hampered the use of both calibrations. According with Groeneveld & Chiessi (2011) discriminate between encrusted and nonencrusted specimens. In core GL-1090 such differentiation would lead to an infeasible number of *G. inflata* shells to perform Mg/Ca analyses. Besides, offsets of up to 7 °C were reported by these authors between the different encrustation states, which could result in large bias adopting this calibration. In Cléroux et al. (2013) did not discriminate between encrusted and nonencrusted *G. inflata* shells, however, they did not apply the cleaning protocol of Barker et al. (2003). Cléroux, Demenocal, et al. (2013) explained that this is likely the reason for the lower pre-exponential constant compared with other calibrations. Consequently, the calibration of Cléroux et al. (2013) resulted in temperatures that we judged unrealistic for the Santos Basin thermocline. For these reasons, we chose the calibration from Cléroux et al. (2008) given by  $[Mg/Ca = 0.71 \exp 0.06 \cdot (T)]$ . This equation was developed using North Atlantic core-tops and was calibrated in an isotopic temperature range (10.5 – 17.9 °C) similar to the one found in the thermocline of the Santos basin. The authors also applied the cleaning protocol of Barker et al. (2003), which generated pre-exponential constant more in line with other equations. Moreover, part of the trace elemental measurements was made on 250 – 315  $\mu m$  (CLÉROUX et al., 2008). This size fraction is near to the one selected in this study, which consequently reduces the error associated with size effect.

The temperature –  $\delta^{18}O$  relationship  $[T = 16.9 - 4.0 (\delta^{18}O_C - \delta^{18}O_{SW})]$  (SHACKLETON, 1974) was applied in order to estimate the seawater  $\delta^{18}O$  composition ( $\delta^{18}O_{SW}$ ) of the thermocline. Here we considered the carbonate *G. inflata*  $\delta^{18}O$  published in (SANTOS et al., 2017b). A conversion factor of 0.27 ‰ was applied to convert the values



from VPDB to Vienna Standard Mean Ocean Water (VSMOW). The effect of changes in global sea level was subtracted from  $\delta^{18}\text{O}_{\text{SW}}$  by applying the sea level correction of Grant et al. (2012). This produced an ice volume-free seawater oxygen isotopic composition ( $\delta^{18}\text{O}_{\text{IVF-SW}}$ ) as a proxy for changes in thermocline salinity.  $\delta^{18}\text{O}_{\text{IVF-SW}}$  error estimation considers an uncertainty of 1.4 °C for the *G. inflata* Mg/Ca calibration (CLÉROUX et al., 2008), which is equivalent to 0.30 ‰  $\delta^{18}\text{O}$  change and an analytical error for *G. inflata*  $\delta^{18}\text{O}$  of 0.06 ‰ (SANTOS et al., 2017b). Hence, the propagated cumulative error estimated for the  $\delta^{18}\text{O}_{\text{IVF-SW}}$  was 0.31 ‰, in line with other studies (e.g. GEBREGIORGIS et al., 2016).

#### 4.1.4 Results

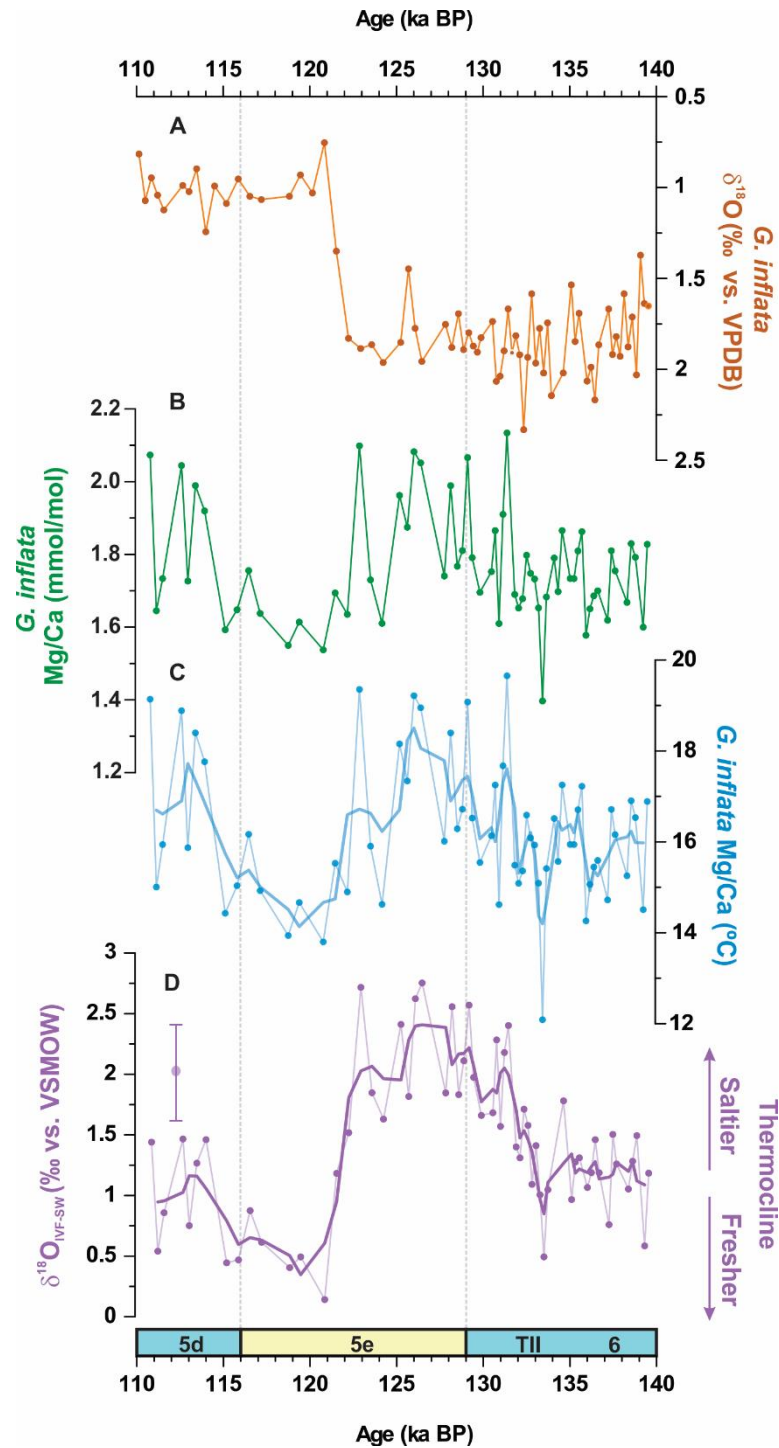
##### 4.1.4.1 Thermocline temperature and ice volume-free seawater oxygen isotopic evolution in the western South Atlantic

Figure 11 presents published *Globorotalia inflata* carbonate  $\delta^{18}\text{O}$  (SANTOS et al., 2017b) and new data related to Mg/Ca concentrations, Mg/Ca-derived temperatures and  $\delta^{18}\text{O}_{\text{IVF-SW}}$  based on *G. inflata* from the core GL-1090, which investigates the period between 160 and 110 ka BP (from the end of the penultimate glacial – MIS 6 – to the last glacial inception – MIS 5d). Mg/Ca concentrations ranged between 2.13 and 1.39 mmol/mol for the studied period (Figure 11b). Thermocline temperatures derived from Mg/Ca were around 16 °C at the end of penultimate glacial (Figure 11c). The main features of our thermocline temperature record are: (i) a progressive warming from TII to early-MIS 5e, reaching maximum values of ca. 18 °C at ca. 126 ka BP; (ii) a drop of 4 °C in temperature after ca. 124 ka BP leading to the coldest thermocline within the studied interval; and (iii) a gradual warming from ca. 116 ka BP during the last glacial inception (MIS 5d), which resulted in temperatures near those of early-MIS 5e (Figure 11c).

A two-phase decrease marked the evolution of thermocline temperatures: firstly between 126 and 124 ka, when the values reduced ca. 2 °C and then after 124 ka when a second drop of more ca. 2 °C occurred. This mid- to late-Last Interglacial pattern characterized the coldest period in the Santos Basin thermocline when temperatures were below 15 °C. At the end of MIS 5e (ca. 117 ka) and more pronounced during glacial inception MIS 5d (after 116 ka), thermocline warmed to values of ca. 18 °C, interrupting the cooling trend that prevailed during the end of the Last Interglacial in the Santos Basin (Figure 11c).

Main changes in thermocline  $\delta^{18}\text{O}_{\text{IVF-SW}}$  followed those of Mg/Ca-derived temperatures. The highest increase occurred from TII to early-MIS 5e, when thermocline  $\delta^{18}\text{O}_{\text{IVF-SW}}$  raised ca. 1.5 ‰, reaching values above 2.0 ‰. After 124 ka, a sharp decrease produced the freshest thermocline for the studied period, when  $\delta^{18}\text{O}_{\text{IVF-SW}}$  was kept between 0.75 and 0.5 ‰ (Figure 11d). During glacial inception MIS 5d, thermocline  $\delta^{18}\text{O}_{\text{IVF-SW}}$  slightly increased to ca. 1.0 ‰ but did not achieve values as high as those recorded during the early-Last Interglacial. According to the Goddard Institute for Space Studies (<http://data.giss.nasa.gov/o18data>), the water depth between 200-400 m delimited by the area of 20°S-30°S and 30°W-40°W presents today an average seawater  $\delta^{18}\text{O}$  of 0.65 ‰. This means that during TII and early-MIS 5e the injection of salty thermocline waters through the Agulhas Leakage (AL), produced a non-analogous South Atlantic Central Water (SACW) in the western South Atlantic. From mid- to late-MIS 5e, i.e., the period that the AL weakened (SANTOS et al., 2017b) and the Atlantic Meridional Overturning Circulation assumed a modern-like configuration (MARINO et al., 2013), the values of our thermocline  $\delta^{18}\text{O}_{\text{IVF-SW}}$  reconstruction resemble those found today in the thermocline.

**Figure 11** - Evolution of Santos Basin thermocline proprieties from the Termination II (TII) to the last glacial inception. A: *Globorotalia inflata* (250 – 300  $\mu\text{m}$ )  $\delta^{18}\text{O}$  ref. 1. B: *Globorotalia inflata* (250 – 300  $\mu\text{m}$ ) Mg/Ca (this study). C: Thermocline temperature derived from *Globorotalia inflata* Mg/Ca applying the calibration equation of Cl  roux et al. (2008) given by  $[\text{Mg}/\text{Ca} = 0.71 \exp 0.06^*(T)]$ . D: Thermocline  $\delta^{18}\text{O}_{\text{IVF-SW}}$  reconstructed with *Globorotalia inflata*  $\delta^{18}\text{O}$  and Mg/Ca temperature. Error bar is relative to  $1\sigma$ . Thermocline temperature and  $\delta^{18}\text{O}_{\text{IVF-SW}}$  (panels C and D) are presented with a three-point running average (thick lines). Grey dashed lines indicate the boundary between Marine Isotope Stage 6-5e and 5e-5d. Marine isotope stages and TII are indicated at the bottom of the panel.



Source: Source: Developed by the author, 2019.

### 4.1.5 Discussion

#### 4.1.5.1 Salinification of the upper subtropical South Atlantic associated with the strengthening of the Agulhas Leakage

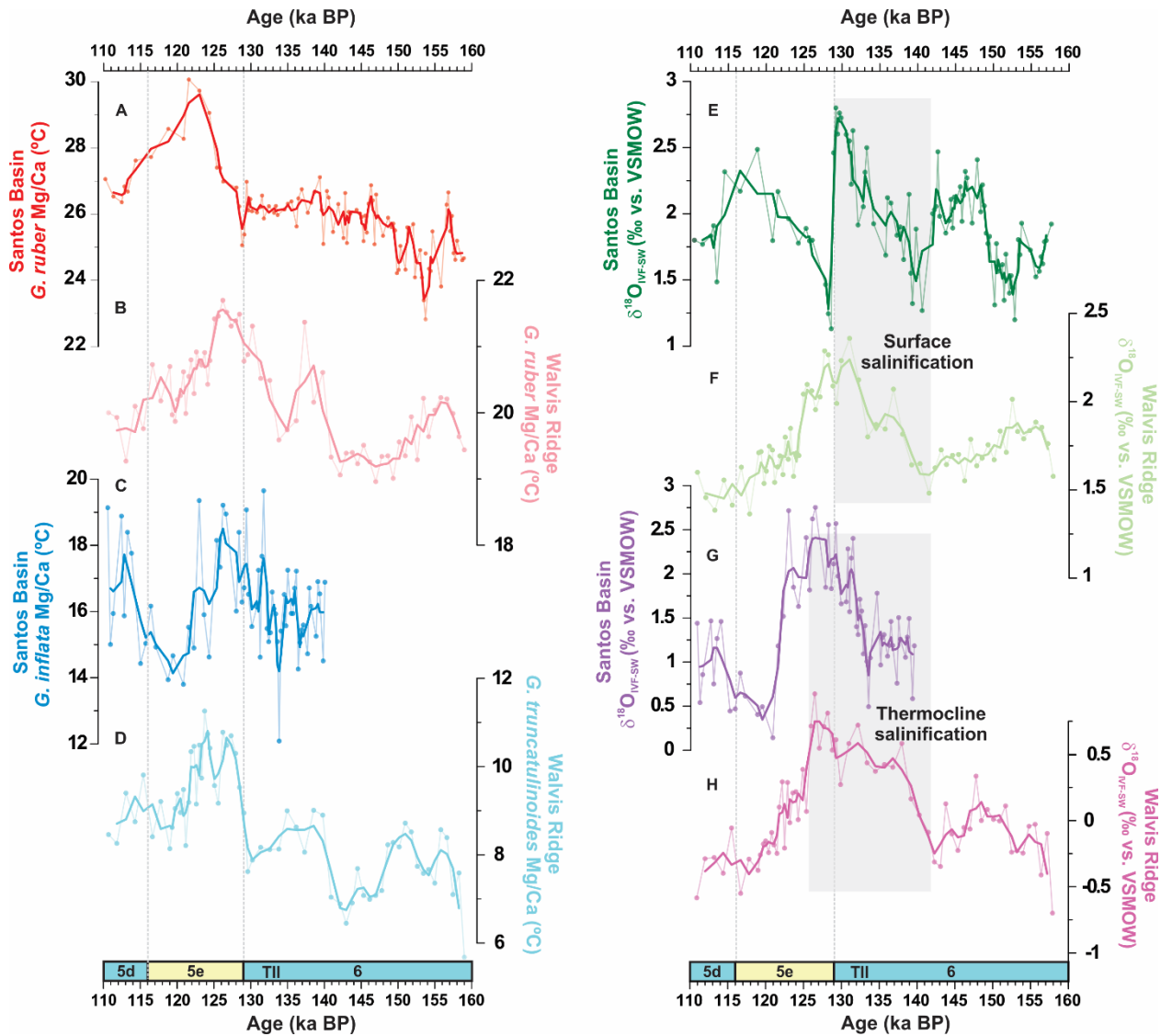
We compare Santos Basin surface and thermocline temperature and  $\delta^{18}\text{O}_{\text{IVF-SW}}$  records from core GL-1090 with those from the Walvis Ridge core 64PE-174P13 (SCUSSOLINI et al., 2015) in order to reconstruct the propagation of the AL signal across the South Atlantic subtropical gyre (Figure 12a-d). The SST records from the Santos Basin (GL-1090) and Walvis Ridge (64PE-174P13) share only a few similarities, suggesting that eastern and western South Atlantic surface temperatures evolved independently between 160 and 110 ka BP (Figure 12a-b). Scussolini et al. (2015) compared the surface temperature between 64PE-174P13 on the Walvis Ridge and more proximal record to AL inflow, MD96-2080 on the Agulhas Bank (MARINO et al., 2013) in the East Atlantic, and also found a few disparities comparing both SST records. This indicates that the input of Indian Ocean (SCUSSOLINI et al., 2015) heat dissipated fast in the surface South Atlantic and could not be recorded further downstream from the AL (Figure 12a-b). The evolution of thermocline temperature between the Santos Basin and Walvis Ridge initially shows more similarities in relation to surface waters, with both records showing warmer values through TII and early-MIS 5e followed by a coeval drop at ca. 124 ka BP (Figure 12c-d). However, thermocline warming registered at the western South Atlantic (GL-1090) during MIS 5d, which is not observed in 64PE-174P13 (Figure 12c and d), indicates that AL is not the only control on Santos Basin thermocline temperatures. Temperature may be more susceptible than salinity to alteration by air-sea interactions and convection along the ring's progression, and therefore the  $\delta^{18}\text{O}_{\text{IVF-SW}}$  may better preserve the signal of the AL strengthening in regions further downstream of the leakage (WEIJER et al., 2001; SCUSSOLINI et al., 2015).

The increase in the Walvis Ridge surface  $\delta^{18}\text{O}_{\text{IVF-SW}}$  starting at ca. 142 ka BP was followed by a near-simultaneous increase in the Santos Basin surface  $\delta^{18}\text{O}_{\text{IVF-SW}}$ . Furthermore, both records show their highest (and thus saltiest) values close to the end of TII (Figure 12e-f). During the period between 160 – 142 ka BP, when the AL was weaker (SCUSSOLINI et al., 2015), the surface  $\delta^{18}\text{O}_{\text{IVF-SW}}$  records exhibit fewer similarities, suggesting that prior to 142 ka BP surface salinities at the Santos Basin and the Walvis Ridge were independently controlled (Figure 12e-f). The fact that cores from both sides of the South Atlantic show an increase in surface salinities from ca. 142 ka BP towards the transition to

MIS 5e, despite their independent age models, suggests a common forcing factor. We propose that the increase in sea surface salinity in the Santos Basin during TII was a response to a basin-wide salinification due to a more vigorous Indian-South Atlantic exchange (Figure 12e-f).

The Santos Basin thermocline  $\delta^{18}\text{O}_{\text{IVF-SW}}$  record suggests that the salty water input likely sourced from the Indian Ocean during the end of MIS 6 was also present below the surface in the western South Atlantic (Figure 12g-h). Unfortunately, the GL-1090 thermocline  $\delta^{18}\text{O}_{\text{IVF-SW}}$  record is not long enough to investigate synchronism in thermocline salinity between the two basins before 142 ka BP. However, two features in the thermocline  $\delta^{18}\text{O}_{\text{IVF-SW}}$  records from GL-1090 and 64PE-174P13 (Walvis Ridge) suggest that they registered basin-wide conditions. First, the peak in thermocline salinity in both cores occurred during MIS 5e at ca. 126 ka BP, later than at the surface (i.e., 129 ka BP) (Figure 12g-h). This shows that the influence of salty waters persisted longer at the thermocline than at the surface. It also suggests that the surface and thermocline circulation responsible for the transfer of salty waters between the eastern and western South Atlantic are not necessarily coupled. In fact, salt anomalies present in the surface eastern South Atlantic may take a more northerly route across the South Atlantic subtropical gyre due to the wind-driven surface circulation, while salt anomalies present in the thermocline may take a more straightforward trajectory to the Santos Basin crossing the central Walvis Ridge (RICHARDSON, 2007). Second, Scussolini et al. (2015) noted that the increase in Walvis Ridge  $\delta^{18}\text{O}_{\text{IVF-SW}}$  was around 70 % larger in the thermocline than at the surface. In the Santos Basin, this proportion was around 80 %. This fact demonstrates that the massive salinification of the thermocline was a conspicuous feature across the subtropical South Atlantic. The good agreement between the surface and thermocline  $\delta^{18}\text{O}_{\text{IVF-SW}}$  records from cores 64PE-174P13 and GL-1090 suggests that AL salty waters flowing through the Walvis Ridge rapidly spread across the South Atlantic subtropical gyre during TII and early-MIS 5e (Figure 12e-h).

**Figure 12** - Evolution of the surface and thermocline eastern (Walvis Ridge) and western (Santos Basin) South Atlantic temperature and ice-volume free seawater stable oxygen isotopic composition ( $\delta^{18}\text{O}_{\text{IVF-SW}}$ ) during the Marine Isotope Stage (MIS) 6/5e transition. A and B: Surface temperatures from cores GL-1090 (A, Santos Basin) (SANTOS et al., 2017a) and 64PE-174P13 (B, Walvis Ridge) (SCUSSOLINI et al., 2015) based on Mg/Ca of *Globigerinoides ruber*. C and D: Thermocline temperatures from cores GL-1090 (C, Santos Basin - this study) and 64PE-174P13 (D, Walvis Ridge) (SCUSSOLINI et al., 2015) based on Mg/Ca of *Globorotalia inflata* and *Globorotalia truncatulinoides*, respectively. E and F: Surface  $\delta^{18}\text{O}_{\text{IVF-SW}}$  from cores GL-1090 (E, Santos Basin) (SANTOS et al., 2017b) and 64PE-174P13 (F, Walvis Ridge) (SCUSSOLINI et al., 2015) estimated through Mg/Ca and  $\delta^{18}\text{O}$  of *G. ruber*. G and H: Thermocline  $\delta^{18}\text{O}_{\text{IVF-SW}}$  from cores GL-1090 (G, Santos Basin - this study) and 64PE-174P13 (H, Walvis Ridge) (SCUSSOLINI et al., 2015) estimated through Mg/Ca and  $\delta^{18}\text{O}$  of *G. inflata* and *G. truncatulinoides*, respectively. All records are depicted by the original data (dots and thin line) and the respective three-point running mean (thick line). Grey vertical dashed lines indicate the boundary between MIS 6/5e and 5e/5d. Grey vertical bars on the right-hand panel highlight the interval of surface and thermocline salinification in the eastern and western South Atlantic. MIS and Termination II (TII) are indicated in the bottom of both panels.



Source: Source: Developed by the author, 2019.

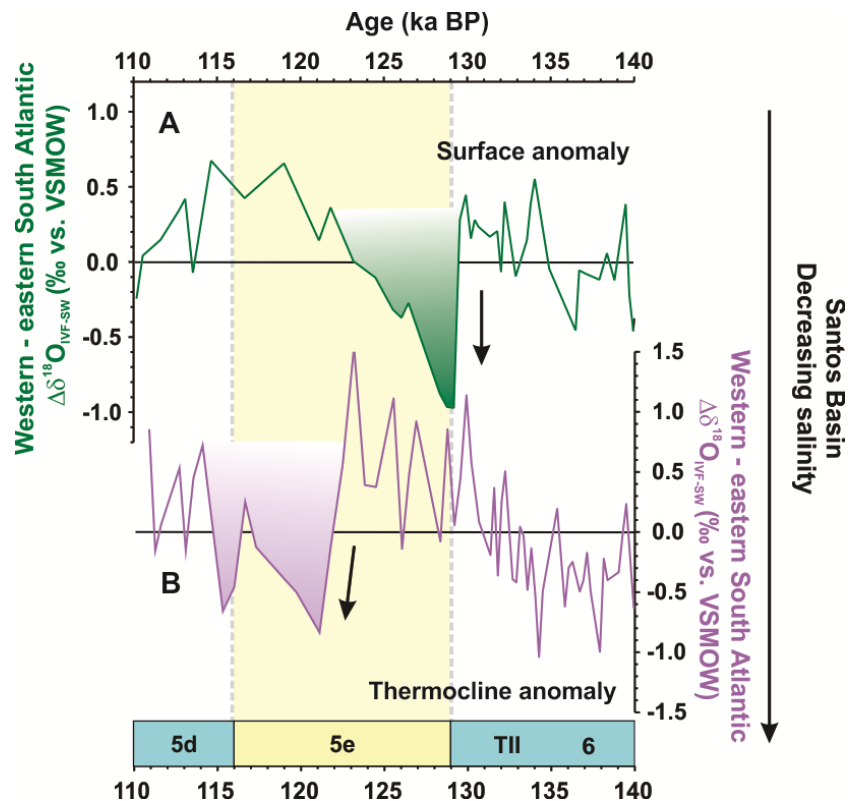
#### 4.1.5.2 Two-phase abrupt freshening of the western South Atlantic and AMOC resumption

The consistent surface and thermocline  $\delta^{18}\text{O}_{\text{IVF-SW}}$  evolution between the eastern and western South Atlantic abruptly breaks down after MIS 5e. Rapid reductions in the  $\delta^{18}\text{O}_{\text{IVF-SW}}$ , first in the surface at ca. 129 ka BP followed by the thermocline at 124 ka BP, illustrate a strong upper ocean freshening of the Santos Basin. Figure 13 exhibits the  $\delta^{18}\text{O}_{\text{IVF-SW}}$  anomaly, the gradient between GL-1090 and 64PE-174P13 (expressed by the  $\Delta\delta^{18}\text{O}_{\text{IVF-SW}}$ ). The strong decrease in the  $\Delta\delta^{18}\text{O}_{\text{IVF-SW}}$  after 129 ka BP and 124 ka BP for the surface and thermocline, respectively, suggests the existence of saltier waters in the eastern margin of the subtropical South Atlantic (Figure 13). Considering that the Last Interglacial was likely characterized by weaker monsoonal precipitation over South America due to lower regional summer insolation (CRUZ et al., 2005) and that the Santos Basin does not receive the discharge of large rivers, it is very unlikely that the surface freshening was the result of direct precipitation or continental freshwater input. Thus, a reorganization of the subtropical South Atlantic circulation is the most plausible explanation for the rapid decrease in upper ocean salinity of the western South Atlantic. Flowing southwards with the BC, these salty waters could reach the regions of the Subtropical Front and eventually be transferred to the Southern Ocean. However, an increase in upper salinity of this region would be contrary to evidence that point towards a lower density of the Southern Ocean during intervals of  $\text{CO}_2$  release from the deep-ocean (ADKINS, 2013; HAYES et al., 2014) around Antarctica like TII. The most likely explanation for the surface freshening, therefore, would be an enhanced export of salty waters to the Northern Hemisphere. A regional recirculation cell within the subtropical gyre with a northward transport in the upper 2000 m (SCHMID, 2014), could have carried these salty waters accumulated for more than 10 kyr to the tropical Atlantic, until they reached the NBC and eventually left the South Atlantic.

Taking into account that cores 64PE-174P13 (SCUSSOLINI et al., 2015) and GL-1090 (this study) record changes in surface  $\delta^{18}\text{O}_{\text{IVF-SW}}$  nearly in-phase, that is, from ca. 142 ka we propose a more straightforward comparison between these records by linearly interpolating data of core 64PE-174P13 and transferring it to the age-scale of core GL-1090. We then proceeded with a zero-mean normalization and subtracted each value of core GL-1090 from the respective value of core 64PE-174P13 to determine the  $\Delta\delta^{18}\text{O}_{\text{IVF-SW}}$  between western and eastern South Atlantic surface and thermocline. This exercise shows that during the Last Interglacial two intervals of abrupt decrease in the  $\Delta\delta^{18}\text{O}_{\text{IVF-SW}}$  turned the Santos Basin relatively fresher compared with Walvis Ridge (Figure 13). We attributed this pattern to

the fact that, while the Santos Basin abruptly lost its salt content due to a strong northward transfer after modifications in the tropical Atlantic ocean-atmosphere configuration, the Walvis Ridge  $\delta^{18}\text{O}_{\text{IVF-SW}}$  shows a more smoother pattern, reflecting the gradual decline in the passage of Agulhas rings by the region. By the time of the last glacial inception (MIS 5d), when the passage of rings was again in a minimum state or might have totally ceased, the Santos basin upper ocean was again saltier. The higher amplitude of the thermocline  $\Delta\delta^{18}\text{O}_{\text{IVF-SW}}$  compared with surface likely reside on the fact that much of the Agulhas signal invades South Atlantic below the surface. However, it is also important to highlight that *G. truncatulinoides* may have a deeper habitat than *G. inflata* and consequently would record a colder and fresher water mass. This greater difference between depth preferences likely also contributes for a higher amplitude of the thermocline  $\Delta\delta^{18}\text{O}_{\text{IVF-SW}}$ .

**Figure 13** -  $\Delta\delta^{18}\text{O}_{\text{IVF-SW}}$  gradient between the upper western and eastern South Atlantic. A: Subtraction of zero-mean normalization of surface  $\delta^{18}\text{O}_{\text{IVF-SW}}$  of core GL-1090 (this study) and 64PE-174P13 (SCUSSOLINI et al., 2015) to generate the  $\Delta\delta^{18}\text{O}_{\text{IVF-SW}}$ . For this case, both cores consider *Globigerinoides ruber* as the suitable species to record surface ocean properties. B: Subtraction of zero-mean normalization of thermocline  $\delta^{18}\text{O}_{\text{IVF-SW}}$  of core GL-1090 (this study) and 64PE-174P13. This estimation takes into account *Globorotalia inflata* for core GL-1090 and *Globorotalia truncatulinoides* for core 64PE-174PE. Either species tend to record the conditions of thermocline, although *G. truncatulinoides* is usually assumed as a deeper thermocline dwelling compared with *G. inflata*. Yellow bar highlights the interval of the Last Interglacial when the two abrupt freshening of the Santos Basin occurred.



Source: Source: Developed by the author, 2019.

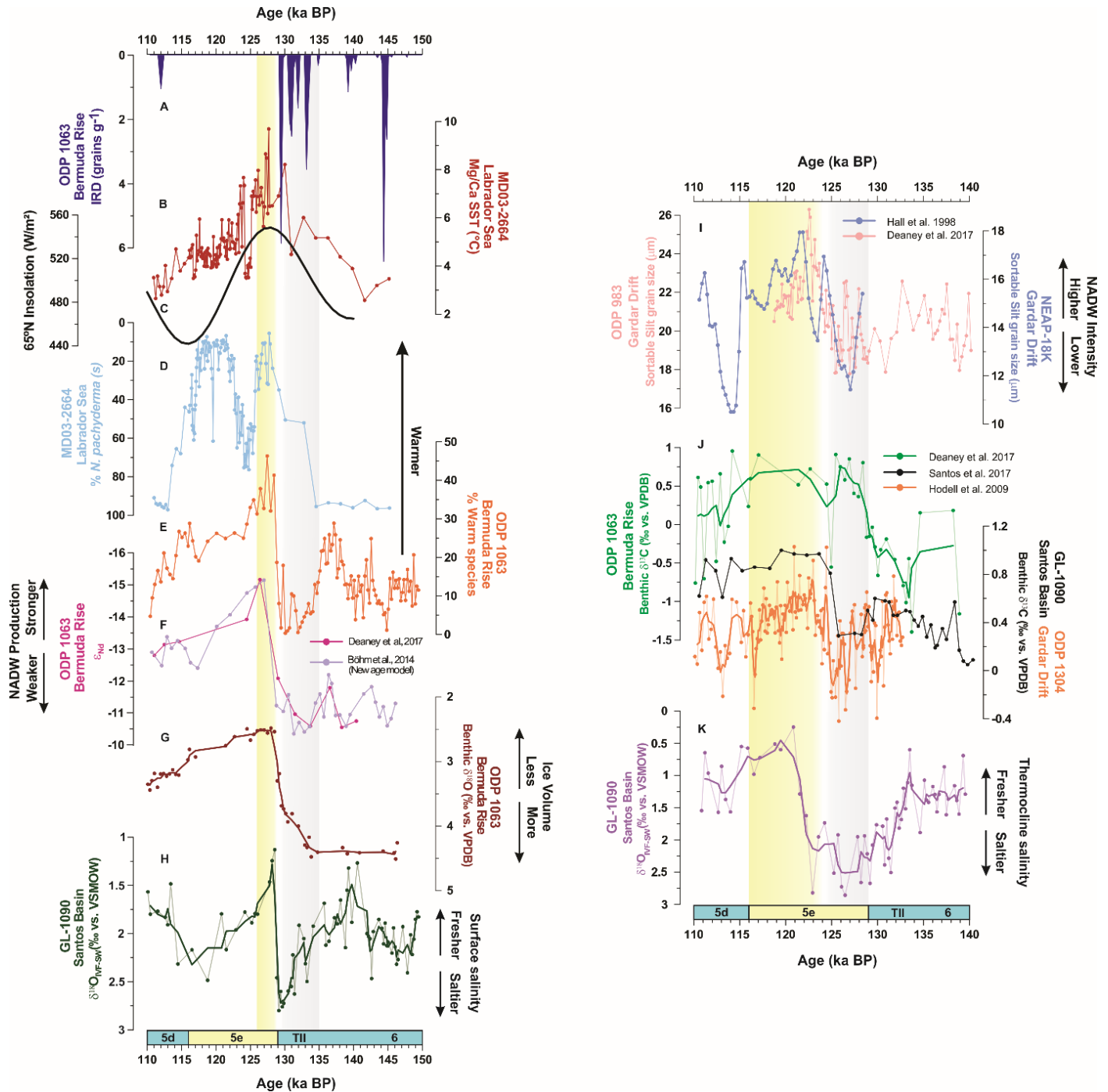


Export of salty waters from the South Atlantic at the beginning of MIS 5e may have had a central role in climate processes in the high latitudes of the North Atlantic. Recent results from the Bermuda Rise (ODP1063), subtropical North Atlantic, show a large and abrupt decrease in benthic  $\delta^{18}\text{O}$  and the presence of very unradiogenic neodymium isotopic values in the deep (4,584 m) North Atlantic at the beginning of MIS 5e (Figure 14f and g) (BÖHM et al., 2015; DEANEY; BARKER; FLIERDT, 2017). These data suggest that the return of deep-water convection following Heinrich stadial (HS) 11 was accomplished by a drastic deepening (overshoot) of deep-waters formed in the northwestern North Atlantic (Labrador Sea), which was initiated at ca. 128.7 ka BP and completed in less than 400 years. The overshoot requires the transfer of salty waters from the tropical Atlantic, accumulated during the end of MIS 6 as a result of a weakened overturning, which entered the southern Labrador Sea and induced hydrostatic instabilities that counterbalanced the influence of low-density meltwater (DEANEY; BARKER; FLIERDT, 2017). The nature of our surface  $\delta^{18}\text{O}_{\text{IVF-SW}}$  record suggests that salty waters from the western South Atlantic may have played a prominent role in restoring deep-ocean convection in the Labrador Sea. Indeed, the similar timing between changes in GL-1090 and ODP1063 supports this suggestion (Figure 14f-h). The abrupt decrease in the Santos Basin surface salinity developed within a short interval (129.1-128.5 ka BP) and occurred right after the end of meltwater influx produced by HS 11 (MARINO et al., 2015) (Figure 14a). Furthermore, the age model of GL-1090 shows the same magnitude of uncertainties as the one from ODP1063 during the transition MIS 6/5e (DEANEY; BARKER; FLIERDT, 2017) (see section 4.1.3.2). Caesar et al. (2018) showed that, at long timescales, deep-ocean convection related to the AMOC is the main factor controlling the surface temperature evolution in the subpolar North Atlantic. Consequently, peak values in surface temperature in core MD03-2664 (IRVALI et al., 2016) from the Eirik Drift, southern Labrador Sea, besides showing a deglacial warming during early MIS 5e, could also be seen as a signal of strong overturning (Figure 14b) (IRVALI et al., 2016; CAESAR et al., 2018). High abundances of warm subtropical species of planktic foraminifera in the Bermuda Rise parallel with decreasing polar species in the Labrador Sea also suggest the progression of warmer and likely saltier Atlantic waters into the subpolar Labrador Sea, which propitiated the AMOC overshoot at ca. 129 ka BP (Figure 14d and e) (IRVALI et al., 2016; DEANEY; BARKER; FLIERDT, 2017). A northern position of the Arctic Front and a stronger and more E-W oriented subpolar gyre would have facilitated the transport of warm and saline subtropical waters to the vicinity of core MD03-2664 (IRVALI et al., 2016). Indeed, the increase in surface  $\delta^{18}\text{O}_{\text{IVF-SW}}$  and peak warmth characterized the transition to the

Last Interglacial in many records of the subpolar North Atlantic (OPPO et al., 2006; GOVIN et al., 2012; MOKEDDEM et al., 2014).

Importantly, the high surface  $\delta^{18}\text{O}_{\text{IVF-SW}}$  waters from the western South Atlantic that flushed into the North Atlantic and eventually propitiated deep-water convection at ca. 129 ka BP probably originated from the AL. However, instead of being rapidly transported from the AL to the North Atlantic, these waters were temporally stored (since ca. 142 ka BP) in the subtropical South Atlantic. The subsequent release of these waters by the western South Atlantic eliminates the large temporal difference between the strengthening of the AL and the effective resumption of deep-water convection (SCUSSOLINI et al., 2015; DEANEY et al., 2017) and gives the immediacy that marine records should present to conciliate the Indian-South Atlantic exchange with glacial-interglacial transitions, at least for TII (Figure 14a-h).

**Figure 14** - Surface and thermocline ice-volume free seawater  $\delta^{18}\text{O}$  ( $\delta^{18}\text{O}_{\text{IVF-SW}}$ ) of the South Atlantic and the Atlantic Meridional Overturning Circulation (AMOC) resumption during the early- and mid-Last Interglacial. A: Ice rafted debris (IRD) from core ODP1063 (DEANEY; BARKER; FLIERDT, 2017). B: Sea surface temperatures (SST) based on Mg/Ca of *Neogloboquadrina pachyderma* (sinistral) from core MD03-2664 (IRVALI et al., 2016). C: June 21 insolation at 65 °N (BERGER, 1978). D: Relative abundance of polar planktic foraminifera *N. pachyderma* (sinistral) from core MD03-2664 (IRVALI et al., 2016). E: Warm planktic foraminifera species (*Globigerinoides ruber* + *Globigerinoides sacculifer*) from core ODP1063 (DEANEY; BARKER; FLIERDT, 2017). F: Neodymium isotopic composition ( $\epsilon\text{Nd}$ ) from core ODP 1063 (pink (DEANEY; BARKER; FLIERDT, 2017) and purple (BÖHM et al., 2015)). G: *Cibicides wuellerstorfi*  $\delta^{18}\text{O}$  from core ODP1063 (DEANEY; BARKER; FLIERDT, 2017). H: Surface  $\delta^{18}\text{O}_{\text{IVF-SW}}$  from core GL-1090 estimated through Mg/Ca and  $\delta^{18}\text{O}$  of *G. ruber* (SANTOS et al., 2017a). I: Sortable silt from cores NEAP-18K (blue) (HALL et al., 1998) and ODP983 (pink) (DEANEY; BARKER; FLIERDT, 2017). J: *C. wuellerstorfi*  $\delta^{13}\text{C}$  from cores ODP1063 (green) (DEANEY; BARKER; FLIERDT, 2017), GL-1090 (black) (SANTOS et al., 2017a) and ODP U1304 (orange) (HODELL et al., 2009). K: Thermocline  $\delta^{18}\text{O}_{\text{IVF-SW}}$  of core GL-1090 estimated through Mg/Ca and  $\delta^{18}\text{O}$  of *Globorotalia inflata* (this study). Marine isotope stages and Termination II (TII) are indicated in the bottom of both panels. Grey and yellow vertical bars indicate the peak in salt accumulation and salt release periods, respectively. Note that grey and yellow bars highlight different periods in the left-hand and right-hand panels.



Source: Source: Developed by the author, 2019.

However, despite the evidence of high SST and an AMOC overshoot due to convection in the Labrador Sea at ca. 129 ka BP (IRVALI et al., 2016; DEANEY et al., 2017) (Figure 14a-h), a modern-like deep Atlantic circulation was only attained later, at ca. 124 ka BP (RASMUSSEN et al., 2003; BAUCH; KANDIANO, 2007; GOVIN et al., 2012; CAPRON et al., 2014). This is shown in Figure 14i-j, where slow current speed estimated by

sortable silt in ODP983 and NEAP-18K and benthic  $\delta^{13}\text{C}$  from IODP Site U1304 (all three records from Gardar Drift, Iceland Basin) (HALL et al., 1998; HODELL et al., 2009; DEANEY; BARKER; FLIERDT, 2017) indicate that deep-water formation in the Nordic Seas did not resume its typical interglacial mode at the beginning of MIS 5e because of the persistent meltwater influence from the Saalian Ice Sheet. Low benthic  $\delta^{13}\text{C}$  of GL-1090 (Santos Basin) (SANTOS et al., 2017a) during early-MIS 5e agrees with that of IODP Site U1304 (HODELL et al., 2009) and suggests that this deep-ocean configuration likely dominated most of the Atlantic basin below depths of  $\sim 2$  km (Figure 14j). The high  $\delta^{13}\text{C}$  only recorded by core ODP1063 (DEANEY; BARKER; FLIERDT, 2017) indicates that the overshoot of deep-water convection at the beginning of MIS 5e in the Labrador Sea neither bathed eastern sites in the North Atlantic basin nor had the necessary impetus to fill the South Atlantic interior (Figure 14j). From ca. 124 ka BP, our data suggest that a secondary release of salty waters from the South Atlantic thermocline (also sourced from the AL), contributed to the return of deep-water convection in the Nordic Seas. This additional salt release provided a load of even denser waters to trigger convection. The drop of more than 2 ‰ in thermocline  $\delta^{18}\text{O}_{\text{IVF-SW}}$  at ca. 124 ka BP in the Santos Basin GL-1090 indicates the transport of salty waters and agrees with benthic  $\delta^{13}\text{C}$  (HODELL et al., 2009; DEANEY; BARKER; FLIERDT, 2017; SANTOS et al., 2017a) and sortable silt from the Gardar Drift (HALL et al., 1998; HODELL et al., 2009), implying the existence of vigorous and stable deep convection from ca. 124 ka BP on (Figure 14i-k).

#### 4.1.5.3 The role of tropical ocean-atmosphere coupling in the Atlantic inter-hemispheric exchange of salt and heat

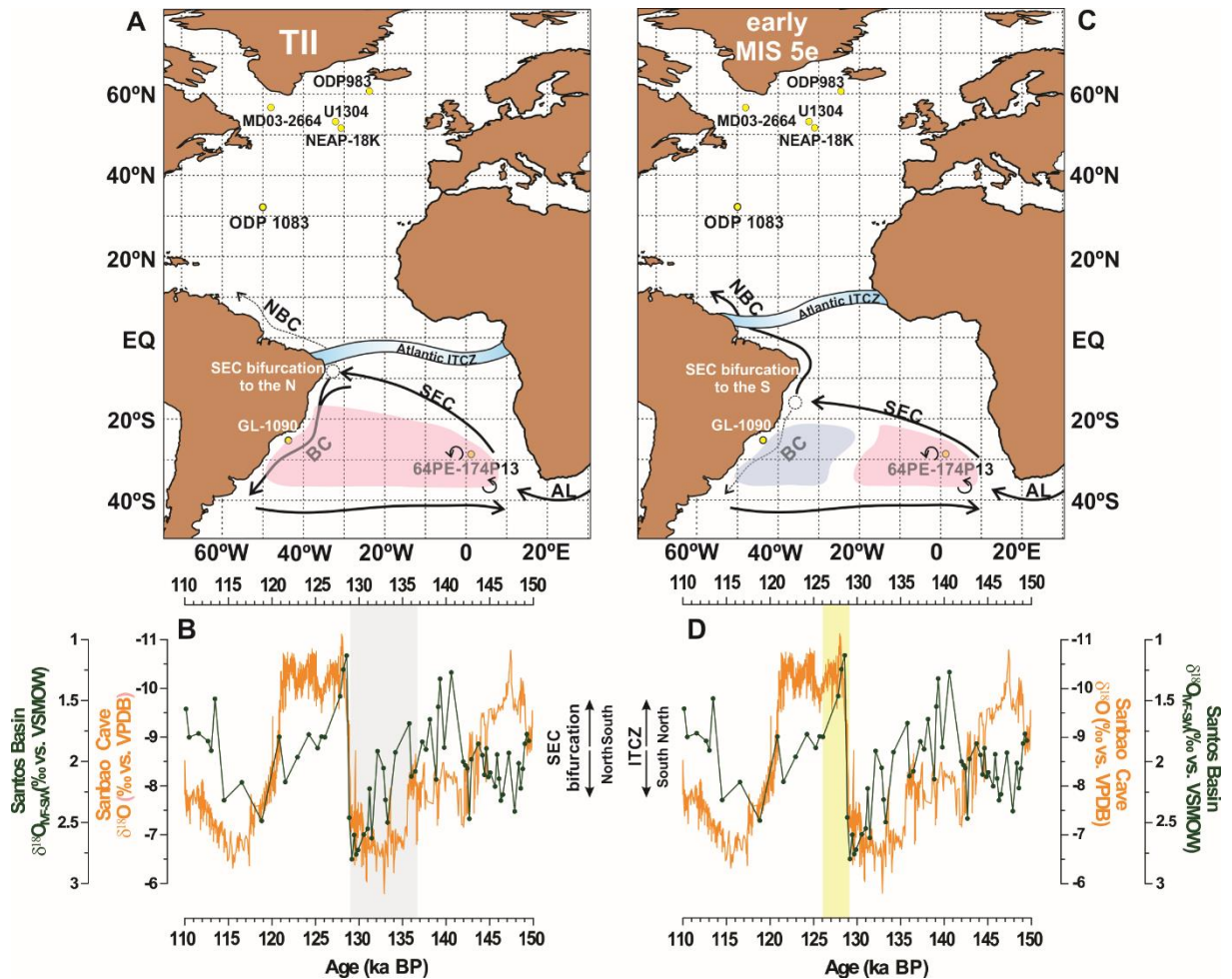
A question arising from our data is if there were dense AL waters available in the South Atlantic since ca. 142 ka BP, why an AMOC resumption did not occur earlier? To answer that question our attention will move to the system responsible for the Atlantic inter-hemispheric salt and heat exchange, namely the bifurcation of the SEC on the eastern South American margin. The SEC bifurcation determines if water masses in the upper South Atlantic become part of the return flow of the meridional overturning or recirculate within the South Atlantic subtropical gyre by favoring either the NBC or the BC, respectively (MARCELLO; WAINER; RODRIGUES, 2018). A numerical simulation demonstrated that the latitude of the SEC bifurcation controls the partitioning of SEC waters entering the NBC

or the BC and is primarily related to variations in the regional wind stress curl associated to the seasonal movement of the Intertropical Convergence Zone (ITCZ) (RODRIGUES; ROTHSTEIN; WIMBUSH, 2007). During austral spring/summer, local positive wind stress curl due to a more southern ITCZ position produces an anomalous anticyclonic circulation, whose southward component near the western boundary of the South Atlantic causes the bifurcation to shift to lower latitudes (RODRIGUES; ROTHSTEIN; WIMBUSH, 2007). This configuration decreases the NBC transport in favor of the BC. A data-model comparison confirmed this suggestion and found a stronger BC when the bifurcation is in its northernmost position at ca. 8 °S during austral summer (SILVA et al., 2009).

A pronounced southward displacement of the Atlantic ITCZ associated with a steep Atlantic meridional SST gradient and a dramatic reduction of the NBC transport are robust climate responses to an AMOC slowdown as shown by model and paleoclimate reconstructions of HS 1 (ZHANG et al., 2011; DEPLAZES et al., 2013; MULITZA et al., 2017) (the strongest AMOC slowdown event of the last deglaciation). It is likely that a similar situation occurred during HS 11, when cold SST dominated the high latitudes of the North Atlantic (IRVALI et al., 2016) shifting the ITCZ to a southern position. Indeed, during HS 11 the East Asian monsoon was markedly reduced (WANG et al., 2008), while very wet conditions prevailed in NE Brazil (WANG et al., 2004). Therefore, we suggest that a southern ITCZ position during the end of the penultimate glacial produced austral spring/summer-like wind stress curl over the surface tropical South Atlantic shifting the SEC bifurcation to a northern position (Figure 15a and b). This ocean-atmosphere coupling worked as a “barrier” enhancing the BC flow and avoiding the cross-equatorial transmission of the salty AL waters that recirculated within the South Atlantic subtropical gyre (Figure 15a). A weaker northward transport of the NBC may have been one of the factors behind the absence of an AMOC resumption during TII (CARLSON, 2008). The redirection of salt anomalies to the BC also explains the uniform evolution of surface and thermocline  $\delta^{18}\text{O}_{\text{IVF-SW}}$  between the Santos Basin and the Walvis Ridge throughout TII (Figure 15e-h). The increase in annual insolation at 65 °N from the end of MIS 6 to early-MIS 5e (BERGER, 1978) (Figure 11c) likely attenuated temperature gradients between high and low latitudes. This change led to a reorganization of the tropical rain belt with a northward shift of the ITCZ (WANG et al., 2008) and, consequently, a southward movement of the SEC bifurcation (Figure 15c and d). Such movement strengthened the NBC and released the salty waters stored in the surface

subtropical gyre of the South Atlantic that contributed to the AMOC overshoot in the Labrador Sea at ca. 129 ka BP (DEANEY; BARKER; FLIERDT, 2017) (Figure 15c).

**Figure 15** - Schematic position of the Intertropical Convergence Zone (ITCZ), the surface circulation of the South Atlantic and sea surface salinity evolution during Termination II (TII) (A and B) and the early Last Interglacial (C and D). Yellow dots show the position of GL-1090 (this study) and other cores discussed here (ODP1058 is not shown). Panels B and D show GL-1090 surface  $\delta^{18}\text{O}_{\text{VFSW}}$  (SANTOS et al., 2017a) together with Sanbao Cave  $\delta^{18}\text{O}$  (WANG et al., 2008) as an indicator of the ITCZ fluctuations across the penultimate glacial-interglacial transition. Note that in A and B the southern ITCZ results in a northern position of the South Equatorial Current (SEC) bifurcation, a stronger Brazil Current (BC), a weaker North Brazil Current (NBC) and the storage of the salty Agulhas Leakage (AL) waters within the South Atlantic subtropical gyre (area in red). The scenario rapidly changed at the onset of the Last Interglacial (C and D) when a northern ITCZ led to a stronger NBC and a weaker BC, decreasing the salinity of the area highlighted in blue.



Source: Source: Developed by the author, 2019.

However, the tardily release of thermocline salty waters by the western South Atlantic at ca. 124 ka BP (Figure 14i-k) calls for processes occurring not only at the sea surface.

Assuming that the ITCZ movements are strongly tied to tropical insolation (HAUG et al., 2001) the shift of the ITCZ to its northernmost position during the Last Interglacial may have been completed only later at ca. 125 ka BP, when annual insolation at 10 °N reached its maximum (BERGER, 1978). Today, the northern and southern hemisphere trade winds associated with the Hadley circulation and ITCZ positioning have a substantial role over the dynamics and latitudinal limits of the North and South Atlantic subtropical cells (GREEN; MARSHALL, 2017). Additionally, the mass transport northward of the AMOC constantly push the North Atlantic subtropical cell to higher latitudes, contributing to the discharge of South Atlantic Central Water into the tropical North Atlantic (KIRCHNER et al., 2009). The northernmost position of the ITCZ likely reached at ca. 125 ka BP promoted these conditions, expanding the South Atlantic subtropical cell northwards. This favored the freshening of the South Atlantic thermocline and produced the 4 °C cooling observed in *G. inflata* Mg/Ca of GL-1090 from ca 124 ka BP (Figure 19e and f). Indeed, the suggested transfer of salt and heat towards the North Atlantic subtropical cell is supported by the similar thermocline salinity and temperature increase indicate by ODP1058 from the Blake Outer Ridge, subtropical North Atlantic (BAHR et al., 2013) (Figure 19c-f). The reverse operation of this mechanism, i.e., a southward displacement of the North Atlantic subtropical cell in periods of weakened overturning, has been proposed to explain a subsurface warming of the tropical North Atlantic during the last deglaciation (SCHMIDT et al., 2012).

Our data show that, in a vigorous state the overturning decreases the salinity and temperature of the western South Atlantic thermocline, fitting the asymmetrical mechanism proposed by Crowley (1992). Intensification in the production of North Atlantic Deep Water would be accompanied by the import of warm waters from the Southern Hemisphere with a polar amplification of the response in the South Atlantic (CROWLEY, 1992). Hence, the interval between ca. 124 and 116 ka BP when fresh and cold conditions dominated the western South Atlantic thermocline preconizes the period of full deep-water convection during MIS 5e and has virtually the same duration of peak interglacial conditions demonstrated by sortable silt (HALL et al., 1998) and polar planktic foraminifera (IRVALI et al., 2016) from the North Atlantic (Figure 19a and b). During this period, thermocline heat was likely transported northwards and released to the surface in regions of strong vertical mixing. Part of this heat may have contributed to sustain a warm climate during the end of MIS 5e under decreasing Northern Hemisphere summer insolation (BORN; NISANCIOGLU; RISEBROBAKKEN, 2011). Importantly, the dynamics of the SEC bifurcation previously

discussed also account for the South Atlantic subtropical cell, since nearly all equatorward thermocline flow passes through the western boundary carried by the NBC flux (MALANOTTE-RIZZOLI et al., 2000). In this way, a southern placement of the SEC bifurcation during the mid-Last Interglacial would favor the release of thermocline salty waters from ca. 124 ka BP yielding dense waters to contribute to deep-water production in the Nordic Seas (HALL et al., 1998; DEANEY; BARKER; FLIERDT, 2017) (Figure 19).

**Figure 16** - South Atlantic thermocline temperature and ice-volume free seawater  $\delta^{18}\text{O}$  ( $\delta^{18}\text{O}_{\text{IVF-SW}}$ ) from Termination II (TII) to the last glacial inception (Marine Isotope Stage 5d) compared with North Atlantic paleoclimate reconstructions. A: Sortable silt from core NEAP-18K (HALL et al., 1998). B: Relative abundance of polar planktic foraminifera *Neogloboquadrina pachyderma* (sinistral) from core MD03-2664 (IRVALI et al., 2016). C: Thermocline temperature from core ODP1058 based on Mg/Ca of *Globorotalia truncatulinoides* (sinistral) (BAHR et al., 2013). D: Thermocline  $\delta^{18}\text{O}_{\text{IVF-SW}}$  from core ODP 1058 estimated through Mg/Ca and  $\delta^{18}\text{O}$  of *G. truncatulinoides* (sinistral) (BAHR et al., 2013). E: Thermocline temperature from core GL-1090 (Santos Basin) based on Mg/Ca of *Globorotalia inflata* (this study). F: Thermocline  $\delta^{18}\text{O}_{\text{IVF-SW}}$  from core GL-1090 estimated through Mg/Ca and  $\delta^{18}\text{O}$  of *G. inflata* (this study). Marine isotope stages and TII are indicated in the bottom of the panel. Yellow bar highlights the period of full deep-water convection in both the Labrador and Nordic Seas. When this condition was achieved salt and heat were removed from the western South Atlantic thermocline.



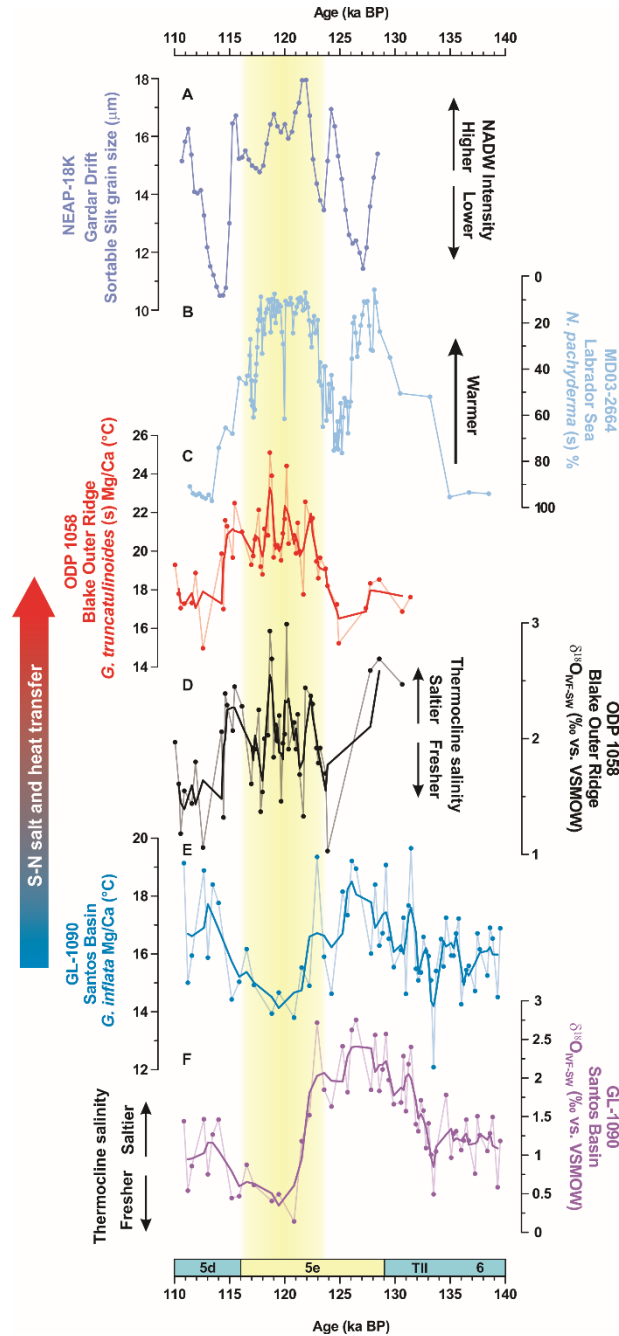


Figure 17 - Source: Source: Developed by the author, 2019.

#### 4.1.6 Conclusions

In summary, the establishment of Last Interglacial climate with a vigorous AMOC occurred in two steps. While the first step produced the resumption of deep convection in the Labrador Sea (IRVALI et al., 2016; DEANEY; BARKER; FLIERDT, 2017) at ca. 129 ka BP, the second step was associated with the onset of deep convection in the Nordic Seas (RASMUSSEN et al., 2003; BAUCH; KANDIANO, 2007; GOVIN et al., 2012) at ca. 124 ka

BP. Our data suggest that salty AL waters were stored in the upper subtropical South Atlantic and released to the North Atlantic in two pulses, supporting this view. Such situation fits the classical “salt oscillator” in which the AMOC is modulated by periods of salt buildup, when the circulation weakens, and salt drain down, when the AMOC resumes (BROECKER et al., 1990). We suggest that the latitude of the SEC bifurcation acted as an ocean gateway, regulating the transfer of buoyancy anomalies introduced to the South Atlantic by the AL. When this gateway strengthened the NBC transport a strong northward flux of salt ensued, propelling deep convection at the high latitudes of the North Atlantic. For the first time we are able to solve the large temporal difference between the strengthening of the AL and the AMOC. Moreover, our data highlight that the AL alone is not enough to reestablish deep-water formation and that a favorable tropical Atlantic ocean-atmosphere configuration must occur to secure the northward transfer of salt.

#### 4.1.7 References

ADKINS, J. F. The role of deep ocean circulation in setting glacial climates. **Paleoceanography**, v. 28, n. 3, p. 539–561, 2013.

ANAND, P.; ELDERFIELD, H.; CONTE, M. H. Calibration of Mg/Ca thermometry in planktonic foraminifera from a sediment trap time series. **Paleoceanography**, v. 18, n. 2, p. 1–15, jun. 2003.

BAHR, A. et al. Millennial-scale versus long-term dynamics in the surface and subsurface of the western North Atlantic Subtropical Gyre during Marine Isotope Stage 5. **Global and Planetary Change**, v. 111, p. 77–87, dez. 2013.

BARD, E.; RICKABY, R. E. M. Migration of the subtropical front as a modulator of glacial climate. **Nature**, v. 460, n. 7253, p. 380–383, jul. 2009.

BARKER, S.; GREAVES, M.; ELDERFIELD, H. A study of cleaning procedures used for foraminiferal Mg/Ca paleothermometry. **Geochemistry, Geophysics, Geosystems**, v. 4, n. 9, p. 1–20, 2003.

BAUCH, H. A.; KANDIANO, E. S. Evidence for early warming and cooling in North Atlantic surface waters during the last interglacial. **Paleoceanography**, v. 22, n. 1, p. 1–11, mar. 2007.

BAZIN, L. et al. An optimized multi-proxy, multi-site Antarctic ice and gas orbital

chronology (AICC2012): 120-800 ka. **Climate of the Past**, v. 9, n. 4, p. 1715–1731, ago. 2013.

BEAL, L. M. et al. The Sources and Mixing Characteristics of the Agulhas Current. **Journal of Physical Oceanography**, v. 36, n. 11, p. 2060–2074, nov. 2006.

BEAL, L. M. et al. On the role of the Agulhas system in ocean circulation and climate. **Nature**, v. 472, n. 7344, p. 429–436, 28 abr. 2011.

BERGER, A. Long-Term Variations of Daily Insolation and Quaternary Climatic Changes. **Journal of the Atmospheric Sciences**, v. 35, n. 12, p. 2362–2367, dez. 1978.

BIASTOCH, A.; BÖNING, C. W.; LUTJEHARMS, J. R. E. Agulhas leakage dynamics affects decadal variability in Atlantic overturning circulation. **Nature**, v. 456, n. 7221, p. 489–492, nov. 2008.

BIASTOCH, A. et al. Increase in Agulhas leakage due to poleward shift of Southern Hemisphere westerlies. **Nature**, v. 462, n. 7272, p. 495–498, nov. 2009.

BLAAUW, M.; CHRISTEN, J. A. Bacon Manual - v2.2. **Tutorial**, p. 1–11, 2013.

BÖHM, E. et al. Strong and deep Atlantic meridional overturning circulation during the last glacial cycle. **Nature**, v. 517, n. 7532, p. 73–76, jan. 2015.

BORN, A.; NISANCIOGLU, K. H.; RISEBROBAKKEN, B. Late Eemian warming in the Nordic Seas as seen in proxy data and climate models. **Paleoceanography**, v. 26, n. 2, p. 1–10, jun. 2011.

BROECKER, W. S. et al. A salt oscillator in the glacial Atlantic? 1. The concept. **Paleoceanography**, v. 5, n. 4, p. 469–477, ago. 1990.

BRYDEN, H. L.; BEAL, L. M.; DUNCAN, L. M. Structure and Transport of the Agulhas Current and Its Temporal Variability. **Journal of Oceanography**, v. 61, n. 3, p. 479–492, jun. 2005.

BYRNE, D. A.; GORDON, A. L.; HAXBY, W. F. Agulhas Eddies: A Synoptic View Using Geosat ERM Data. **Journal of Physical Oceanography**, v. 25, n. 5, p. 902–917, maio 1995.

CAESAR, L. et al. Observed fingerprint of a weakening Atlantic Ocean overturning circulation. **Nature**, v. 556, n. 7700, p. 191–196, abr. 2018.

CALEY, T. et al. Agulhas leakage as a key process in the modes of Quaternary climate changes. **Proceedings of the National Academy of Sciences**, v. 109, n. 18, p. 6835–6839, maio 2012.

CALEY, T. et al. Quantitative estimate of the paleo-Agulhas leakage. **Geophysical Research Letters**, v. 41, n. 4, p. 1238–1246, 28 fev. 2014.

CAPRON, E. et al. Temporal and spatial structure of multi-millennial temperature changes at high latitudes during the Last Interglacial. **Quaternary Science Reviews**, v. 103, p. 116–133, nov. 2014.

CARLSON, A. E. Why there was not a Younger Dryas-like event during the Penultimate Deglaciation. **Quaternary Science Reviews**, v. 27, n. 9–10, p. 882–887, maio 2008.

CHIESSI, C. M. et al. Signature of the Brazil-Malvinas Confluence (Argentine Basin) in the isotopic composition of planktonic foraminifera from surface sediments. **Marine Micropaleontology**, v. 64, n. 1–2, p. 52–66, 2007.

CLÉROUX, C. et al. Deep-dwelling foraminifera as thermocline temperature recorders. **Geochemistry, Geophysics, Geosystems**, v. 8, n. 4, p. 1-19, abr. 2007.

CLÉROUX, C. et al. Mg/Ca and Sr/Ca ratios in planktonic foraminifera: Proxies for upper water column temperature reconstruction. **Paleoceanography**, v. 23, n. 3, p.1-16, set. 2008.

CLÉROUX, C. et al. Reconstructing the upper water column thermal structure in the Atlantic Ocean. **Paleoceanography**, v. 28, n. 3, p. 503–516, 2013.

CORTESE, G.; ABELMANN, A.; GERSONDE, R. The last five glacial-interglacial transitions: A high-resolution 450,000-year record from the subantarctic Atlantic. **Paleoceanography**, v. 22, n. 4, p. 1-14, dez. 2007.

CROWLEY, T. J. North Atlantic Deep Water cools the southern hemisphere. **Paleoceanography**, v. 7, n. 4, p. 489–497, ago. 1992.

CRUZ, F. W. et al. Insolation-driven changes in atmospheric circulation over the past 116,000 years in subtropical Brazil. **Nature**, v. 434, n. 7029, p. 63–66, mar. 2005.

CUNNINGHAM, S. A. et al. Temporal Variability of the Atlantic Meridional Overturning Circulation at 26.5 N. **Science**, v. 317, n. 5840, p. 935–938, ago. 2007.

DE RUIJTER, W. P. M. et al. Indian-Atlantic interocean exchange: Dynamics, estimation and impact. **Journal of Geophysical Research: Oceans**, v. 104, n. C9, p. 20885–20910, set. 1999.

DEANEY, E. L.; BARKER, S.; FLIERDT, T. VAN DE. Timing and nature of AMOC recovery across Termination 2 and magnitude of deglacial CO<sub>2</sub> change. **Nature Communications**, Published online: 27 February 2017; | doi:10.1038/ncomms14595, v. 8, p. 14595, 2017.

DEPLAZES, G. et al. Links between tropical rainfall and North Atlantic climate during the last glacial period. **Nature Geoscience**, v. 6, n. 3, p. 213–217, 2013.

DOGLIOLI, A. M. et al. A Lagrangian analysis of the Indian-Atlantic interocean exchange in a regional model. **Geophysical Research Letters**, v. 33, n. 14, p. L14611, 2006.

ELDERFIELD, H.; GANSEN, G. Past temperature and  $\delta^{18}\text{O}$  of surface ocean waters inferred from foraminiferal Mg/Ca ratios. **Nature**, v. 405, n. 6785, p. 442–445, maio 2000.

GARZOLI, S. L.; MATANO, R. The South Atlantic and the Atlantic Meridional Overturning Circulation. **Deep Sea Research Part II: Topical Studies in Oceanography**, v. 58, n. 17–18, p. 1837–1847, set. 2011.

GEBREGIORGIS, D. et al. South Asian summer monsoon variability during the last ~54 kyrs inferred from surface water salinity and river runoff proxies. **Quaternary Science Reviews**, v. 138, p. 6–15, abr. 2016.

GORDON, A. L. South Atlantic thermocline ventilation. **Deep Sea Research Part A. Oceanographic Research Papers**, v. 28, n. 11, p. 1239–1264, nov. 1981.

GORDON, A. L. Indian-Atlantic Transfer of Thermocline Water at the Agulhas Retroflexion. **Science**, v. 227, n. 4690, p. 1030–1033, 1 mar. 1985.

GORDON, A. L. et al. Thermocline and intermediate water communication between the south Atlantic and Indian oceans. **Journal of Geophysical Research**, v. 97, n. C5, p. 7223, 1992.

GOVIN, A. et al. Persistent influence of ice sheet melting on high northern latitude climate during the early Last Interglacial. **Climate of the Past**, v. 8, n. 2, p. 483–507, mar. 2012.

GOVIN, A. et al. Terrigenous input off northern South America driven by changes in

Amazonian climate and the North Brazil Current retroflection during the last 250 ka. **Climate of the Past**, v. 10, n. 2, p. 843–862, abr. 2014.

GRANT, K. M. et al. Rapid coupling between ice volume and polar temperature over the past 150,000 years. **Nature**, v. 491, n. 7426, p. 744–747, nov. 2012.

GREAVES, M. et al. Accuracy, standardization, and interlaboratory calibration standards for foraminiferal Mg/Ca thermometry. **Geochemistry, Geophysics, Geosystems**, v. 6, n. 2, p. 1–9, fev. 2005.

GREEN, B.; MARSHALL, J. Coupling of Trade Winds with Ocean Circulation Damps ITCZ Shifts. **Journal of Climate**, v. 30, n. 12, p. 4395–4411, jun. 2017.

GROENEVELD, J.; CHIESSI, C. M. Mg/Ca of *Globorotalia inflata* as a recorder of permanent thermocline temperatures in the South Atlantic. **Paleoceanography**, v. 26, n. 2, p. 1–12, 2011.

HALL, I. R. et al. Coherent deep flow variation in the Iceland and American basins during the last interglacial. **Earth and Planetary Science Letters**, v. 164, n. 1–2, p. 15–21, dez. 1998.

HAUG, G. H. et al. Southward Migration of the Intertropical Convergence Zone Through the Holocene. **Science**, v. 293, n. 5533, p. 1304–1308, ago. 2001.

HAYES, C. T. et al. A stagnation event in the deep South Atlantic during the last interglacial period. **Science**, v. 346, n. 6216, p. 1514–1517, dez. 2014.

HODELL, D. A. et al. Surface and deep-water hydrography on Gardar Drift (Iceland Basin) during the last interglacial period. **Earth and Planetary Science Letters**, v. 288, n. 1–2, p. 10–19, out. 2009.

IRVALI, N. et al. Evidence for regional cooling, frontal advances, and East Greenland Ice Sheet changes during the demise of the last interglacial. **Quaternary Science Reviews**, v. 150, p. 184–199, out. 2016.

JOHANN R. E. LUTJEHARMS. **The Agulhas Current**. [s.l.] Springer Berlin Heidelberg, 2006.

KASPER, S. et al. Kasper et al 2014 - Salinity changes in the Agulhas leakage area recorded by stable hydrogen isotopes of C37 alkenones during Termination I and II. **Climate of the Past**, v. 10, n. 1, p. 251–260, fev. 2014.

KIRCHNER, K. et al. On the spreading of South Atlantic Water into the Northern Hemisphere. **Journal of Geophysical Research**, v. 114, n. C5, p. C05019, maio 2009.

KUHLBRODT, T. et al. On the driving processes of the Atlantic meridional overturning circulation. **Reviews of Geophysics**, v. 45, n. 2, p. RG2001, abr. 2007.

KUHNERT, H. et al. Holocene tropical western Indian Ocean sea surface temperatures in covariation with climatic changes in the Indonesian region. **Paleoceanography**, v. 29, n. 5, p. 423–437, maio 2014.

LEA, D. W.; PAK, D. K.; PARADIS, G. Influence of volcanic shards on foraminiferal Mg/Ca in a core from the Galápagos region. **Geochemistry, Geophysics, Geosystems**, v. 6, n. 11, p. 1–13, nov. 2005.

LISIECKI, L. E.; RAYMO, M. E. A Pliocene-Pleistocene stack of 57 globally distributed benthic  $\delta^{18}\text{O}$  records. **Paleoceanography**, v. 20, n. 1, mar. 2005.

LONČARIĆ, N. et al. Oxygen isotope ecology of recent planktic foraminifera at the central Walvis Ridge (SE Atlantic). **Paleoceanography**, v. 21, n. 3, set. 2006.

LOULERGUE, L. et al. Orbital and millennial-scale features of atmospheric  $\text{CH}_4$  over the past 800,000 years. **Nature**, v. 453, n. 7193, p. 383–386, maio 2008.

MALANOTTE-RIZZOLI, P. et al. Water mass pathways between the subtropical and tropical ocean in a climatological simulation of the North Atlantic ocean circulation. **Dynamics of Atmospheres and Oceans**, v. 32, n. 3–4, p. 331–371, ago. 2000.

MARCELLO, F.; WAINER, I.; RODRIGUES, R. R. South Atlantic Subtropical Gyre Late Twentieth Century Changes. **Journal of Geophysical Research: Oceans**, v. 123, n. 8, p. 5194–5209, ago. 2018.

MARINO, G. et al. Agulhas salt-leakage oscillations during abrupt climate changes of the Late Pleistocene. **Paleoceanography**, v. 28, n. 3, p. 599–606, set. 2013.

MARINO, G. et al. Bipolar seesaw control on last interglacial sea level. **Nature**, v. 522, n. 7555, p. 197–201, jun. 2015.

MCKENNA, V. S.; PRELL, W. L. Calibration of the Mg/Ca of *Globorotalia truncatulinoides* (R) for the reconstruction of marine temperature gradients. **Paleoceanography**, v. 19, n. 2, p.

1-12, jun. 2004.

MOKEDDEM, Z.; MCMANUS, J. F.; OPPO, D. W. Oceanographic dynamics and the end of the last interglacial in the subpolar North Atlantic. **Proceedings of the National Academy of Sciences**, v. 111, n. 31, p. 11263–11268, ago. 2014.

MORARD, R. et al. Worldwide genotyping in the planktonic foraminifer *globobulimina inflata*: Implications for life history and paleoceanography. **PLoS ONE**, v. 6, n. 10, 2011.

MULITZA, S. et al. Synchronous and proportional deglacial changes in Atlantic meridional overturning and northeast Brazilian precipitation. **Paleoceanography**, v. 32, n. 6, p. 622–633, jun. 2017.

OPPO, D. W.; MCMANUS, J. F.; CULLEN, J. L. Evolution and demise of the Last Interglacial warmth in the subpolar North Atlantic. **Quaternary Science Reviews**, v. 25, n. 23–24, p. 3268–3277, dez. 2006.

PEETERS, F. J. C. et al. Vigorous exchange between the Indian and Atlantic oceans at the end of the past five glacial periods. **Nature**, v. 430, n. 7000, p. 661–665, ago. 2004.

PETERSON, R. G.; STRAMMA, L. Upper-level circulation in the South-Atlantic Ocean. **Progress In Oceanography**, v. 26, n. 1, p. 1–73, 1991.

RASMUSSEN, T. L. et al. Late warming and early cooling of the sea surface in the Nordic seas during MIS 5e (Eemian Interglacial). **Quaternary Science Reviews**, v. 22, n. 8–9, p. 809–821, abr. 2003.

REGENBERG, M. et al. Calibrating Mg/Ca ratios of multiple planktonic foraminiferal species with  $\delta^{18}\text{O}$ -calcification temperatures: Paleothermometry for the upper water column. **Earth and Planetary Science Letters**, v. 278, n. 3–4, p. 324–336, fev. 2009.

RICHARDSON, P. L. Agulhas leakage into the Atlantic estimated with subsurface floats and surface drifters. **Deep Sea Research Part I: Oceanographic Research Papers**, v. 54, n. 8, p. 1361–1389, ago. 2007.

RIDGWAY, K. R.; DUNN, J. R. Observational evidence for a Southern Hemisphere oceanic supergyre. **Geophysical Research Letters**, v. 34, n. 13, p. 1–5, 16 jul. 2007.

RODRIGUES, R. R.; ROTHSTEIN, L. M.; WIMBUSH, M. Seasonal Variability of the South Equatorial Current Bifurcation in the Atlantic Ocean: A Numerical Study. **Journal of Physical Oceanography**, v. 37, n. 1, p. 16–30, jan. 2007.



SANTOS, T. P. et al. Prolonged warming of the Brazil Current precedes deglaciations. **Earth and Planetary Science Letters**, v. 463, n. April, p. 1–12, 2017a.

SANTOS, T. P. et al. The Impact of the AMOC Resumption in the Western South Atlantic Thermocline at the Onset of the Last Interglacial. **Geophysical Research Letters**, v. 44, n. 22, p. 11,547–11,554, nov. 2017b.

SCHMID, C. **Mean vertical and horizontal structure of the subtropical circulation in the South Atlantic from three-dimensional observed velocity fields**. [s.l.] Elsevier, 2014. v. 91

SCHMIDT, M. W. et al. Impact of abrupt deglacial climate change on tropical Atlantic subsurface temperatures. **Proceedings of the National Academy of Sciences**, v. 109, n. 36, p. 14348–14352, set. 2012.

SCUSSOLINI, P. et al. Saline Indian Ocean waters invaded the South Atlantic thermocline during glacial termination II. **Geology**, v. 43, n. 2, p. 139–142, fev. 2015.

SHACKLETON, N. J. Attainment of isotopic equilibrium between ocean water and the benthonic foraminifera geus *Uvigerina*: Isotopic changes in the ocean during the last glacial. **Colloques Internationaux du C.N.R.S.**, v. 219, p. 203–210, 1974.

SILVA, M. et al. High-resolution regional ocean dynamics simulation in the southwestern tropical Atlantic. **Ocean Modelling**, v. 30, n. 4, p. 256–269, jan. 2009.

SONG, Q.; GORDON, A. L.; VISBECK, M. Spreading of the Indonesian Throughflow in the Indian Ocean\*. **Journal of Physical Oceanography**, v. 34, n. 4, p. 772–792, abr. 2004.

STRAMMA, L.; ENGLAND, M. On the water masses and mean circulation of the South Atlantic Ocean. **Journal of Geophysical Research: Oceans**, v. 104, n. C9, p. 20863–20883, set. 1999.

VAN AKEN, H. M. et al. Observations of a young Agulhas ring, Astrid, during MARE in March 2000. **Deep Sea Research Part II: Topical Studies in Oceanography**, v. 50, n. 1, p. 167–195, jan. 2003.

VAN SEBILLE, E. et al. Flux comparison of Eulerian and Lagrangian estimates of Agulhas leakage: A case study using a numerical model. **Deep Sea Research Part I: Oceanographic Research Papers**, v. 57, n. 3, p. 319–327, mar. 2010.

VAN SEBILLE, E. et al. Ocean currents generate large footprints in marine palaeoclimate proxies. **Nature Communications**, v. 6, n. 1, p. 6521, 4 dez. 2015.

VAN SEBILLE, E.; VAN LEEUWEN, P. J. Fast Northward Energy Transfer in the Atlantic due to Agulhas Rings. **Journal of Physical Oceanography**, v. 37, n. 9, p. 2305–2315, set. 2007.

VERES, D. et al. The Antarctic ice core chronology (AICC2012): an optimized multi-parameter and multi-site dating approach for the last 120 thousand years. **Climate of the Past**, v. 9, n. 4, p. 1733–1748, ago. 2013.

WANG, X. et al. Wet periods in northeastern Brazil over the past 210 kyr linked to distant climate anomalies. **Nature**, v. 432, n. 7018, p. 740–743, dez. 2004.

WANG, Y. et al. Millennial- and orbital-scale changes in the East Asian monsoon over the past 224,000 years. **Nature**, v. 451, n. 7182, p. 1090–1093, fev. 2008.

WEIJER, W. Response of the Atlantic overturning circulation to South Atlantic sources of buoyancy. **Global and Planetary Change**, v. 34, n. 3–4, p. 293–311, nov. 2002.

WEIJER, W.; DE RUIJTER, W. P. M.; DIJKSTRA, H. A. Stability of the Atlantic Overturning Circulation: Competition between Bering Strait Freshwater Flux and Agulhas Heat and Salt Sources. **Journal of Physical Oceanography**, v. 31, n. 8, p. 2385–2402, ago. 2001.

ZHANG, D. et al. Multidecadal variability of the North Brazil Current and its connection to the Atlantic meridional overturning circulation. **Journal of Geophysical Research**, v. 116, n. C4, p. C04012, abr. 2011.

## 5 GENERAL CONCLUSIONS AND FUTURE PERSPECTIVES

In summary, the scientific contribution of this work was done with a multi-proxy interpretation around the Last Interglacial period that suggests an efficient transport toward the northern Hemisphere and, hence AMOC overshooting, increasing salt and heat due AL intensification is observed in the South Atlantic subtropical gyre. This salty anomaly was abruptly released northward in two-phases and fed both sites of NADW production, firstly at 129 ka the Labrador Sea and then at 124 ka in the Nordic Sea. The proposed mechanism suggests a favorable ocean-atmospheric configuration is needed to release the salty anomaly

from tropical South Atlantic and to induce deep-water convection in high latitudes. Additionally, GL-1090 data reaffirms that Indo-Atlantic exchange performed by AL is fundamental to reestablish the South Atlantic thermohaline circulation during TII. However, there is lack of records spanning the TII close to the equatorial region or positioned close to SEC bifurcation, on the CNB trajectory, in which agrees with Ballalai et al. (2019, in the revision) and propose investigate the mechanism associated to salt and heat transport to the establishment of an interglacial climate. In this sense, the core GL-1180 is positioned at  $\sim 8^\circ\text{S}$  and has a relative low sedimentation rate, covering at least the last three Terminations. The already ongoing Ph.D. project using another sediment core close to the Equatorial region, GL-1180 core allows going further on the mechanism proposed here, and its role on the deglaciation process, as well as the role of AL on glacial Terminations. However, there is an impasse in the scientific community about the real contribution of AL to STG and its role on the energy transport toward northern hemisphere.

As can be seen in this work, the increase in the South Atlantic-Indian Ocean exchange might be detected by the changes in upper ocean temperature and salinity induced by the AL. These changes in surface and thermocline waters in Santos Basin reflect the hydrographic response of AL evolution path toward the South Atlantic subtropical gyre. In general, the STG acts as a conduit to warm and saline waters from AL, known as warm-water route (Indo-Atlantic connection). Meanwhile, comparatively cold and less saline waters from Antarctic Circumpolar Current are known as cold-water route (Pacific-Atlantic connection), which flows into South Atlantic through the Drake Passage. In this way, although the contribution of these two routes can impact the thermohaline circulation due to its different properties, there is not a consensus about the predominance and relative contribution of these two routes on STG, hence on AMOC transport.

Different studies show that there is a divergence between those who support the greater contribution of the warm-water route (e.g., SPEICH; BLANKE; MADEC, 2001) to the STG and those who support the idea that the cold-water route (e.g., MACDONALD, 1998) is the dominant route and the one that most influences the waters of the STG. The volumetric contribution of the different sources and their respective trajectories within the STG make interpretations difficult mainly due to the potential modification of their signals along their trajectory, although the properties of thermohaline circulation are well known. This behavior may have a significant influence under STG and consequently in AMOC, but there are still uncertainties about the real role of the South Atlantic on the inter-hemispheric communication. The fact is that the South Atlantic behaves not only as a passive conductor of

water bodies, but it actively influences through different processes such ocean-atmospheric interactions, mixture, subduction, and advective processes along its course (GARZOLI; MATANO, 2011).

In this sense, despite the work contribution in understanding the role of AL and the mechanisms that precede deglaciation processes that are needed to the establishment of an interglacial climate, the real contribution of the STG is still doubtful and needs further investigations. Further researches approaching the warm and cold routes of the STG will contribute to understand the role of the South Atlantic subtropical gyre on northward energy transport as well as its role as an inter-oceanic connector that feeds the AMOC.

## 6 REFERENCES

- ANAND, P.; ELDERFIELD, H.; CONTE, M. H. Calibration of Mg/Ca thermometry in planktonic foraminifera from a sediment trap time series. **Paleoceanography**, v. 18, n. 2, p. 1-15, jun. 2003.
- ANDERSON, D. M. Paleocanography. **Encyclopedia of Quaternary Science**, p. 1599–1609, 2007.
- BARD, E. Hydrological Impact of Heinrich Events in the Subtropical Northeast Atlantic. **Science**, v. 289, n. 5483, p. 1321–1324, ago. 2000.
- BARD, E.; RICKABY, R. E. M. Migration of the subtropical front as a modulator of glacial climate. **Nature**, v. 460, n. 7253, p. 380–383, jul. 2009.
- BARKER, S. et al. Interhemispheric Atlantic seesaw response during the last deglaciation. **Nature**, v. 457, n. 7233, p. 1097–1102, fev. 2009.
- BASSINOT, F. C. Oxygen Isotope Stratigraphy of the Oceans. **Encyclopedia of Quaternary Science**, v. 18, n. 2000, p. 1740–1748, 2007.
- BEAL, L. M. et al. On the role of the Agulhas system in ocean circulation and climate. **Nature**, v. 472, n. 7344, p. 429–436, 28 abr. 2011.
- BIASTOCH, A.; BÖNING, C. W.; LUTJEHARMS, J. R. E. Agulhas leakage dynamics affects decadal variability in Atlantic overturning circulation. **Nature**, v. 456, n. 7221, p. 489–492, nov. 2008.
- BIASTOCH, A. et al. Variability and Coherence of the Agulhas Undercurrent in a High-Resolution Ocean General Circulation Model. **Journal of Physical Oceanography**, v. 39, n. 10, p. 2417–2435, out. 2009a.
- BIASTOCH, A. et al. Increase in Agulhas leakage due to poleward shift of Southern

Hemisphere westerlies. **Nature**, v. 462, n. 7272, p. 495–498, nov. 2009b.

BIASTOCH, A.; BÖNING, C. W. Anthropogenic impact on Agulhas leakage. **Geophysical Research Letters**, v. 40, n. 6, p. 1138–1143, 2013.

BÖHM, E. et al. Strong and deep Atlantic meridional overturning circulation during the last glacial cycle. **Nature**, v. 517, n. 7532, p. 73–76, jan. 2015.

BROECKER, W. S. Paleocean circulation during the 1st deglaciation: A bipolar seesaw? **Paleoceanography**, v. 13, n. 2, p. 119–121, 1998.

BRYDEN, H. L.; LONGWORTH, H. R.; CUNNINGHAM, S. A. Slowing of the Atlantic meridional overturning circulation at 25° N. **Nature**, v. 438, n. 7068, p. 655–657, dez. 2005.

BUIZERT, C.; SCHMITTNER, A. Southern Ocean control of glacial AMOC stability and Dansgaard-Oeschger interstadial duration. **Paleoceanography**, v. 30, n. 12, p. 1595–1612, 2015.

BYRNE, D. A.; GORDON, A. L.; HAXBY, W. F. Agulhas Eddies: A Synoptic View Using Geosat ERM Data. **Journal of Physical Oceanography**, v. 25, n. 5, p. 902–917, maio 1995.

CALEY, T. et al. Agulhas leakage as a key process in the modes of Quaternary climate changes. **Proceedings of the National Academy of Sciences**, v. 109, n. 18, p. 6835–6839, maio 2012.

CALEY, T. et al. Quantitative estimate of the paleo-Agulhas leakage. **Geophysical Research Letters**, v. 41, n. 4, p. 1238–1246, fev. 2014.

CARLSON, A. E. et al. Subtropical Atlantic salinity variability and Atlantic meridional circulation during the last deglaciation. **Geology**, v. 36, n. 12, p. 991–994, 2008.

CLARK, P. U. et al. The role of the thermohaline circulation in abrupt climate change. **Nature**, v. 415, n. 6874, p. 863–869, fev. 2002.

CLÉROUX, C. et al. Deep-dwelling foraminifera as thermocline temperature recorders. **Geochemistry, Geophysics, Geosystems**, v. 8, n. 4, p. 1-19, abr. 2007.

CLÉROUX, C. et al. Mg/Ca and Sr/Ca ratios in planktonic foraminifera: Proxies for upper water column temperature reconstruction. **Paleoceanography**, v. 23, n. 3, p. 1-16, set. 2008.

CLÉROUX, C. et al. Reconstructing the upper water column thermal structure in the Atlantic Ocean. **Paleoceanography**, v. 28, n. 3, p. 503–516, set. 2013.

CORTESE, G.; ABELMANN, A.; GERSONDE, R. The last five glacial-interglacial transitions: A high-resolution 450,000-year record from the subantarctic Atlantic. **Paleoceanography**, v. 22, n. 4, p. 1-14, dez. 2007.

CRONIN, M. F. et al. **Monitoring Ocean - Atmosphere Interactions in Western Boundary Current Extensions**. Proceedings of OceanObs'09: Sustained Ocean Observations and

Information for Society. **Anais...**European Space Agency, dez. 2010. Disponível em: <<http://www.oceanobs09.net/proceedings/cwp/cwp20>>

CROWLEY, T. J. North Atlantic Deep Water cools the southern hemisphere. **Paleoceanography**, v. 7, n. 4, p. 489–497, ago. 1992.

DE RUIJTER, W. P. M. et al. Indian-Atlantic interocean exchange: Dynamics, estimation and impact. **Journal of Geophysical Research: Oceans**, v. 104, n. C9, p. 20885–20910, set. 1999.

DEKENS, P. S. et al. Core top calibration of Mg/Ca in tropical foraminifera: Refining paleotemperature estimation. **Geochemistry, Geophysics, Geosystems**, v. 3, n. 4, p. 1–29, abr. 2002.

DOGLIOLI, A. M. et al. A Lagrangian analysis of the Indian-Atlantic interocean exchange in a regional model. **Geophysical Research Letters**, v. 33, n. 14, p. L14611, 2006.

DONG, B.-W.; SUTTON, R. T. Adjustment of the coupled ocean-atmosphere system to a sudden change in the Thermohaline Circulation. **Geophysical Research Letters**, v. 29, n. 15, p. 18-1-18-4, ago. 2002.

DONNERS, J.; DRIJFHOUT, S. S. The Lagrangian View of South Atlantic Interocean Exchange in a Global Ocean Model Compared with Inverse Model Results. **Journal of Physical Oceanography**, v. 34, n. 5, p. 1019–1035, maio 2004.

DYEZ, K. A.; ZAHN, R.; HALL, I. R. Multicentennial Agulhas leakage variability and links to North Atlantic climate during the past 80,000 years. **Paleoceanography**, v. 29, n. 12, p. 1238–1248, dez. 2014.

EMILIANI, C. Pleistocene Temperatures. **The Journal of Geology**, v. 63, n. 6, p. 538–578, nov. 1955.

EMILIANI, C. Isotopic Paleotemperatures. **Science**, v. 154, n. 3751, p. 851–857, nov. 1966.

GARZOLI, S. L. Geostrophic velocity and transport variability in the Brazil-Malvinas Confluence. **Deep Sea Research Part I: Oceanographic Research Papers**, v. 40, n. 7, p. 1379–1403, 1993.

GARZOLI, S. L. et al. Three Agulhas rings observed during the Benguela Current Experiment. **Journal of Geophysical Research: Oceans**, v. 104, n. C9, p. 20971–20985, set. 1999.

GARZOLI, S. L. et al. South Atlantic meridional fluxes. **Deep Sea Research Part I: Oceanographic Research Papers**, v. 71, p. 21–32, jan. 2013.

GARZOLI, S. L.; MATANO, R. The South Atlantic and the Atlantic Meridional Overturning Circulation. **Deep Sea Research Part II: Topical Studies in Oceanography**, v. 58, n. 17–18, p. 1837–1847, set. 2011.

GETZLAFF, J. Signal propagation related to the North Atlantic overturning. **Geophysical Research Letters**, v. 32, n. 9, p. L09602, 2005.

GONI, G. J.; BRINGAS, F.; DINEZIO, P. N. Observed low frequency variability of the Brazil Current front. **Journal of Geophysical Research**, v. 116, n. C10, p. C10037, out. 2011.

GORDON, A. L. Indian-Atlantic Transfer of Thermocline Water at the Agulhas Retroflection. **Science**, v. 227, n. 4690, p. 1030–1033, mar. 1985.

GORDON, A. L. Interocean exchange of thermocline water. **Journal of Geophysical Research**, v. 91, n. C4, p. 5037, 1986.

GORDON, A. L. Brazil-Malvinas Confluence–1984. **Deep Sea Research Part A. Oceanographic Research Papers**, v. 36, n. 3, p. 359–384, 1989.

GORDON, A. L. et al. Thermocline and intermediate water communication between the south Atlantic and Indian oceans. **Journal of Geophysical Research**, v. 97, n. C5, p. 7223, 1992.

GROENEVELD, J.; CHIESSI, C. M. Mg/Ca of *Globorotalia inflata* as a recorder of permanent thermocline temperatures in the South Atlantic. **Paleoceanography**, v. 26, n. 2, p. 1–12, 2011.

JOHANN R. E. LUTJEHARMS. **The Agulhas Current**. [s.l.] Springer Berlin Heidelberg, 2006.

JOHNSON, H. L.; MARSHALL, D. P. A Theory for the Surface Atlantic Response to Thermohaline Variability. **Journal of Physical Oceanography**, v. 32, n. 4, p. 1121–1132, abr. 2002.

KASPER, S. et al. Salinity changes in the Agulhas leakage area recorded by stable hydrogen isotopes of C37 alkenones during Termination I and II. **Climate of the Past**, v. 10, n. 1, p. 251–260, 2014.

KATZ, M. E. et al. Traditional and emerging geochemical proxies in foraminifera. **The Journal of Foraminiferal Research**, v. 40, n. 2, p. 165–192, abr. 2010.

KNORR, G.; LOHMANN, G. Rapid transitions in the Atlantic thermohaline circulation triggered by global warming and meltwater during the last deglaciation. **Geochemistry, Geophysics, Geosystems**, v. 8, n. 12, p. 1–22, dez. 2007.

LEA, D. W.; MASHIOTTA, T. A.; SPERO, H. J. Controls on magnesium and strontium uptake in planktonic foraminifera determined by live culturing. **Geochimica et Cosmochimica Acta**, v. 63, n. 16, p. 2369–2379, ago. 1999.

MACDONALD, A. M. The global ocean circulation: a hydrographic estimate and regional analysis. **Progress in Oceanography**, v. 41, n. 3, p. 281–382, jun. 1998.

MARCELLO, F.; WAINER, I.; RODRIGUES, R. R. South Atlantic Subtropical Gyre Late

Twentieth Century Changes. **Journal of Geophysical Research: Oceans**, v. 123, n. 8, p. 5194–5209, ago. 2018.

MARINO, G. et al. Agulhas salt-leakage oscillations during abrupt climate changes of the Late Pleistocene. **Paleoceanography**, v. 28, n. 3, p. 599–606, set. 2013.

MCMANUS, J. F. et al. High-resolution climate records from the North Atlantic during the last interglacial. **Nature**, v. 371, n. 6495, p. 326–329, set. 1994.

MCMANUS, J. F. et al. Collapse and rapid resumption of Atlantic meridional circulation linked to deglacial climate changes. **Nature**, v. 428, n. 6985, p. 834–837, abr. 2004.

MOROS, M. et al. Were glacial iceberg surges in the North Atlantic triggered by climatic warming? **Marine Geology**, v. 192, n. 4, p. 393–417, dez. 2002.

MULITZA, S. et al. The South Atlantic Carbon Isotope Record of Planktic Foraminifera. In: FISCHER, G.; WEFER, G. (Eds.). . **Use of Proxies in Paleoceanography**. Berlin, Heidelberg: Springer Berlin Heidelberg, 1999. p. 427–445.

MULITZA, S. et al. Sahel megadroughts triggered by glacial slowdowns of Atlantic meridional overturning. **Paleoceanography**, v. 23, n. 4, p. 1–11, dez. 2008.

MURRAY-WALLACE, C. V. SEA LEVEL STUDIES | Eustatic Sea-Level Changes – Glacial–Interglacial Cycles. In: **Encyclopedia of Quaternary Science**. [s.l.] Elsevier, 2013. p. 429–438.

OLSON, D. B. et al. Temporal variations in the separation of Brazil and Malvinas Currents. **Deep Sea Research Part A. Oceanographic Research Papers**, v. 35, n. 12, p. 1971–1990, dez. 1988.

PEETERS, F. J. C. et al. Vigorous exchange between the Indian and Atlantic oceans at the end of the past five glacial periods. **Nature**, v. 430, n. 7000, p. 661–665, ago. 2004.

PETERSON, R. G.; STRAMMA, L. Upper-level circulation in the South-Atlantic Ocean. **Progress In Oceanography**, v. 26, n. 1, p. 1–73, 1991.

RAHMSTORF, S. Ocean circulation and climate during the past 120,000 years. **Nature**, v. 419, n. 6903, p. 207–214, set. 2002.

RICHARDSON, P. L. Agulhas leakage into the Atlantic estimated with subsurface floats and surface drifters. **Deep Sea Research Part I: Oceanographic Research Papers**, v. 54, n. 8, p. 1361–1389, ago. 2007.

RITZ, S. P. et al. Estimated strength of the Atlantic overturning circulation during the last deglaciation. **Nature Geoscience**, v. 6, n. 3, p. 208–212, fev. 2013.

SCHMIDT, M. W.; SPERO, H. J.; LEA, D. W. Links between salinity variation in the Caribbean and North Atlantic thermohaline circulation. **Nature**, v. 428, n. 6979, p. 160–163, mar. 2004.



- SIJP, W. P.; ENGLAND, M. H. Southern Hemisphere Westerly Wind Control over the Ocean's Thermohaline Circulation. **Journal of Climate**, v. 22, n. 5, p. 1277–1286, mar. 2009.
- SILVEIRA, I. C. A. DA et al. A corrente do Brasil ao largo da costa leste brasileira. **Revista Brasileira de Oceanografia**, v. 48, n. 2, p. 171–183, 2000.
- SPEICH, S.; BLANKE, B.; MADEC, G. Warm and cold water routes of an O.G.C.M. thermohaline conveyor belt. **Geophysical Research Letters**, v. 28, n. 2, p. 311–314, jan. 2001.
- SPERO, H. J. et al. Multispecies approach to reconstructing eastern equatorial Pacific thermocline hydrography during the past 360 kyr. **Paleoceanography**, v. 18, n. 1, p. 1–16, mar. 2003.
- STEPH, S. et al. Stable isotopes of planktonic foraminifera from tropical Atlantic/Caribbean core-tops: Implications for reconstructing upper ocean stratification. **Marine Micropaleontology**, v. 71, n. 1–2, p. 1–19, abr. 2009.
- STOCKER, T. F.; JOHNSEN, S. J. A minimum thermodynamic model for the bipolar seesaw. **Paleoceanography**, v. 18, n. 4, p. 1–9, 2003.
- TOGGWEILER, J. R.; RUSSELL, J. L.; CARSON, S. R. Midlatitude westerlies, atmospheric CO<sub>2</sub>, and climate change during the ice ages. **Paleoceanography**, v. 21, n. 0032, jun. 2006.
- VAN SEBILLE, E. et al. Flux comparison of Eulerian and Lagrangian estimates of Agulhas leakage: A case study using a numerical model. **Deep Sea Research Part I: Oceanographic Research Papers**, v. 57, n. 3, p. 319–327, mar. 2010.
- WEIJER, W. Response of the Atlantic overturning circulation to South Atlantic sources of buoyancy. **Global and Planetary Change**, v. 34, n. 3–4, p. 293–311, nov. 2002.
- WEIJER, W.; DE RUIJTER, W. P. M.; DIJKSTRA, H. A. Stability of the Atlantic Overturning Circulation: Competition between Bering Strait Freshwater Flux and Agulhas Heat and Salt Sources. **Journal of Physical Oceanography**, v. 31, n. 8, p. 2385–2402, ago. 2001.
- WELDEAB, S.; SCHNEIDER, R. R.; KÖLLING, M. Deglacial sea surface temperature and salinity increase in the western tropical Atlantic in synchrony with high latitude climate instabilities. **Earth and Planetary Science Letters**, v. 241, n. 3–4, p. 699–706, jan. 2006.
- WEN, C.; CHANG, P.; SARAVANAN, R. Effect of Atlantic Meridional Overturning Circulation Changes on Tropical Atlantic Sea Surface Temperature Variability: A 2½-Layer Reduced-Gravity Ocean Model Study. **Journal of Climate**, v. 23, n. 2, p. 312–332, jan. 2010.
- YIN, J. et al. Big Jump of Record Warm Global Mean Surface Temperature in 2014–2016 Related to Unusually Large Oceanic Heat Releases. **Geophysical Research Letters**, v. 45, n. 2, p. 1069–1078, jan. 2018.